Circulation pattern controls of summer temperature anomalies in southern Africa

Chibuike Chiedozie Ibebuchi *[1,2], Cameron C. Lee[1,2]

[1] *Department of Geography, Kent State University, Kent, Ohio, USA*

[2] *ClimRISE Lab, Kent State University, Kent, Ohio, USA*

**Corresponding author's email:* cibebuch@kent.edu

Abstract

This study investigates the relationship between circulation patterns and austral summer temperature anomalies in southern Africa. The results show that the formation of continental lows tends to increase the partial atmospheric layer thickness. Further, the distinct variabilities of high and low pressure under the circulation types, influence air mass advection from the adjacent oceans, as well as atmospheric stability over land. Stronger anticyclonic circulation at the western branch of the Mascarene high enhances low-level cold air advection by southeast winds, decreases thickness, and lowers the temperature over a majority of the land in southern Africa. Conversely, a weaker Mascarene high, coupled with enhanced cyclonic activity in the southwest Indian Ocean increases low-level warm air advection and increases temperature anomalies over vast regions in southern Africa. The ridging of a closed South Atlantic anticyclone at the southern coast of southern Africa results in colder temperatures in the tip of southern Africa due to enhanced low-level cold air advection by southeast winds. However, when the ridge is weak and westerly winds dominate the southern coast of southern Africa, temperature increases in these areas. The northward track of the Southern Hemisphere mid-latitude cyclone, which can be linked to the negative Southern Annular Mode, reduces the temperature in the southwestern part of southern Africa. Also, during the analysis period, El Niño and the positive Subtropical Indian Ocean dipole were associated with temperature increases over the central parts of southern Africa; while the positive Indian Ocean dipole was linked to a temperature increase over the northeastern, northwestern, and southwestern parts of southern Africa.

Keywords: temperature, circulation types, Subtropical Indian Ocean dipole, Southern Annular Mode, El Niño, Indian Ocean dipole, Mascarene high, South Atlantic anticyclone

Highlights

1. The spatiotemporal variations of temperature over southern Africa are coupled with large-scale circulation patterns modulating warm and cold air advection.
2. Climate drivers heterogeneously influence temperature over the land in southern Africa through control of regional circulation patterns.

https://doi.org/10.1007/s00376-023-2392-3

1. Introduction

Rising global temperatures resulting from both anthropogenic emissions and natural variability impact virtually all aspects of livelihood, ranging from mortality rate (Lee and Sheridan, 2018; Sheridan and Dixon, 2017) and labor productivity (Knittel et al., 2020) to the rate and magnitude of climate extremes (Alimonti et al., 2022), among others. Climate predictions and projections are important for mitigating the consequences of rising temperatures by enhancing preparedness against extreme climate events as well as developing climate policies against future dangerous climate change. A major challenge in forecasting climate events, such as extreme temperatures, stems from the incomplete understanding of the physical mechanisms that drive the climate (Flato et al., 2014). Therefore, there is a need for studies that aim to improve the understanding of the atmospheric processes that govern the earth's climate. Enhanced knowledge of the atmospheric processes that govern the climate can serve as a benchmark for improving climate forecasts. In the regional context of southern Africa, which is vulnerable to anthropogenic climate change due to its economic conditions and geographical location at the descent region of the Hadley circulation (Baudoin et al., 2017), this study aims to enhance the understanding of the large scale circulations that modulate the summer temperatures in southern Africa.

Several studies have hinted at the role of climate drivers in modulating atmospheric circulations over southern Africa (Dieppois et al., 2015; Hoell et al., 2015; Lyon and Mason, 2007; Malherbe et al., 2014; Manatsa et al., 2017; Reason and Rouault, 2005) and other regions in the globe (Pirhalla et al., 2022). Among the climate drivers, the sea surface temperature (SST) patterns of the Subtropical Indian Ocean Dipole (SIOD) and the Southern Annular Mode (SAM) have a direct impact on the climate of southern Africa because they exist in the mid-latitude oceans of the Southern hemisphere (i.e., the subtropical Indian Ocean, and the Southern Ocean). In addition, the Indian Ocean Dipole (IOD) and the El Niño Southern Oscillation (ENSO) have a remote influence on the climate of southern Africa (Reason and Jagadheesha, 2005). Moreover, the imprint of the ENSO signal can be found in the SAM, IOD and SIOD modes since all the climate drivers generally influence SST anomalies in the southwest Indian Ocean as well as the anticyclonic circulation of the Mascarene high. (Ding et al., 2012; Ibebuchi, 2021; Morioka et al., 2015). Therefore, this study also investigates the impact of the climate drivers on temperature variability in southern Africa.

The link between synoptic circulations and precipitation in southern Africa has been widely documented (Burls et al., 2019; Engelbrecht et al., 2015; Engelbrecht and Landman, 2016; Lennard and Hegerl, 2015; Mahlalela et al., 2019; Wolski et al., 2018). Also, studies have highlighted the possible impact of the SAM on temperature anomalies in southern Africa. For example, using regression analysis, (Gillett et al., 2006) investigated the impact of positive SAM on temperatures in the Southern Hemisphere (with the inclusion of southern Africa), however, the negative SAM was not considered and the associating physical processes were not analyzed in detail. Also for other regions in the Southern Hemisphere, such as Australia and

South America, studies have addressed the relationship between the SAM and surface temperatures (Hendon et al., 2007; Silvestri and Vera, 2009). Further, the majority of available works of literature on the IOD and SIOD, with regard to the climate of southern Africa, focus on the relationship between the climate drivers and rainfall variability in southern Africa (Behera and Yamagata, 2001; Hoell et al., 2015; Ibebuchi, 2023; Reason, 2001), and less attention is given to temperature. Given that these climate drivers impact the amplitude and frequency of circulation types (CTs), this study goes further to decompose in time, the distinct circulations in southern Africa and then analyze the mechanisms through which the individual CTs impact surface temperature and relative humidity (that contributes to heat stress) in southern Africa. Thus, the major added value of this study to the literature is the improved understanding of the physical processes through which large-scale circulations influence the spatial variations and magnitude of summer temperatures in southern Africa.

This study is structured as follows, Section 2 presents the data and methods the study is based on; the results are presented in Section 3; Section 4 contains the discussion of the results and conclusions.

2 Data and methodology

2.1 Data

High-resolution reanalysis data is obtained from ERA5 (Hersbach et al., 2020). The ERA5 reanalysis data sets obtained are sea level pressure (SLP); 850 hPa wind vectors, relative humidity, specific humidity, 850 hPa geopotential height; and 1000 hPa geopotential height. Gridded observed 2 m average temperature is obtained from the Climate Prediction Center (CPC) Global Unified Temperature dataset (https://psl.noaa.gov/data/gridded/data.cpc.globaltemp.html). All data sets are obtained at daily temporal resolution from 1979 to 2021. The horizontal resolution of the ERA5 reanalysis data is 0.25° longitude and latitude, and 0.5° longitude and latitude for the gridded CPC 2 m temperature data. Also, correspondence between ERA5 and gridded CPC temperature data has been reported (Roffe and van der Walt, 2023), which strengthens the choice of using both data sets for our analysis.

2.2 Methodology

This current study is incremental work from previous research that applied circulation typing to study circulations in southern Africa at multiple spatial scales (Ibebuchi, 2023a), hence the same classified CTs are used. A major advancement in this study is that these same CTs are now being used to investigate the mechanisms through which circulation patterns modulate the magnitude and spatial variations of austral summer (i.e., December to February – DJF) *temperature* in southern Africa. We consider austral summer as that is when absolute temperatures are highest in the study region, and thus, most impactful. The spatial extent for the CT classification is 0° to 50.25°S and 5.25°E to 55.25°E (Fig. 1). The adjacent maritime regions that act as moisture sources to the landmass were included. Further, when the CTs are linked to temperature over the landmass, typically, to make a distinction with the tropical landmass, southern Africa might be defined to include landmass from about 10°S and poleward. Nonetheless, we have included the tropical latitudes (i.e., up to 0° latitude) to capture variability in the cross-equatorial northeast trade winds. This is because the cross-equatorial northeast trade winds play a role in defining convergence in the Angola Low and the Mozambique

Channel that both impact the climate of southern Africa. However, we focus our analysis on the temperature anomalies under the distinct CTs on land from 10°S and poleward.

The obliquely rotated T-mode (variable is time series and observation is grid points) principal component analysis (Compagnucci and Richman, 2008) applied in a fuzzy approach is used for the classification of the CTs. The details of the classification approach are given in Appendix A. The classification of the CTs with rotated T-mode PCA is a time decomposition technique. Singular value decomposition is applied to the correlation matrix containing the correlation between the SLP fields at the distinct daily time series in the analysis period. The resulting PC loadings which designate the amplitude of the set of circulation patterns at a given day is used to assign CT(s) within the signal range to a given day, which imply the CTs that occurred on the day in question.

We apply map composting of different climate variables to examine the relationship between the classified CTs and DJF temperatures in southern Africa. We have used SLP composites to investigate the horizontal variations of pressure under each of the CTs, which can also be suitable for characterizing continental heating (i.e., in areas with continental lows) as well as atmospheric stability at the boundary layer, and convective activity over the adjacent oceans. We defined the thickness of the atmospheric layer as the vertical distance in meters between two the 1000 hPa and 850 hPa pressure levels. This is because, we found that from iterative pre-evaluations, relatively, the thickness layer values between 1000 hPa and 850 hPa accurately capture the spatiotemporal variations of 2 m mean temperature values in the study region. Thus, we define thickness as the difference between the height at 850 hPa and the height at 1000 hPa. Positive thickness values are related to positive temperature anomalies and negative thickness values are related to negative temperature anomalies. In addition to analyzing the SLP and atmospheric layer thickness, composites of 850 hPa (that is, the height above the eastern escarpment of southern Africa) winds are analyzed to establish the prevailing winds under each CT. Thus, analyzing the SLP, wind directions, and thickness enables documenting low-level cold and warm air advection under each CT.

Given the high seasonality of temperature, to enable a robust diagnosis of the temperature values and other variables used to diagnose temperature patterns under each CT, we rely on composite anomaly values during DJF. The composite anomaly is calculated as the difference between the days assigned to a CT and the 1981-2010 DJF climatology of the variable in question. Regression analysis was used to investigate, at each grid point in the region of assessment, the association between climate drivers (SAM, ENSO, IOD and SIOD) and temperature variability in southern Africa. The statistical significance of the association, based on the regression model, is tested at a 95% confidence level. To control for false discovery rate in the multiple hypothesis testing, we used the Benjamini-Hochberg procedure (Benjamini and Yekutieli, 2001), which assumes that the hypotheses being tested are independent.

3 Results

The standardized SLP composites for the days when the classified CTs occurred during the analysis period are shown in Figure 1. The CTs in Figure 1 were externally validated using SLP data from a different reanalysis product (Ibebuchi 2022c) and a suite of CMIP6 general circulation models (Ibebuchi 2022b). While the CTs are not confined to occur in any specific season, the spatiotemporal structure and dynamics of the CTs can also be influenced by seasonal variations in large-scale processes such as diabatic heating, thus the CTs tend to be dominant in specific seasons when the prevailing (seasonal) atmospheric condition favors their mechanisms (Fig. A1). Pressure variations over the adjacent oceans are used to infer convective activity in these locations – anticyclonic (cyclonic) circulations over the oceans imply suppressed (enhanced) convection. Similarly, pressure variations over the landmass can be used to infer continental heating or atmospheric stability at the boundary layer – anticyclonic (cyclonic) circulations over the land imply a relatively stable (unstable) atmosphere.

Next, for the classified CTs in Fig. 1, we look at the composite anomaly patterns of DJF atmospheric layer thickness between 1000 hPa to 850 hPa (Fig. 2a), temperature (Fig. 2b), and 850 hPa relative humidity (Fig. 3); and composite patterns of 850 hPa wind vectors (Fig. 4). These figures will be interpreted coherently, based on the asymmetric patterns of the CTs (i.e., the positive phase and the negative phase). We focus our analysis of the composite anomaly maps in Figs 2 to 3 mostly on the regions (i.e., group of grid points) with robust changes.

Generally, the composite patterns reveal that under each CT, the DJF temperature anomalies are characterized by spatial heterogeneity (Fig. 2b). A possible explanation for the spatial heterogeneity of temperature anomalies under each CT can be due to the distinct regional climates in southern Africa. Under the asymmetry of each CT (i.e., the negative and positive phases) temperature variations are least in the deep tropics (10°S – 0°) mostly because diabatic heating (and SLP) have fewer variations in the deep tropics. However, as noted earlier, the major focus of the temperature anomalies is on southern Africa. Fig. 2a indicates that for the asymmetry of a given CT, and depending on the circulation features, there appear to be coherent temperature patterns in the central parts of southern Africa – mostly at landmasses close to the southwest Indian Ocean - at the southwestern parts of southern Africa, characterized by the Mediterranean type of climate, and at the southern tip of southern Africa. Thus, the regional climate types of the aforementioned regions contribute to defining the overall spatial heterogeneity of the temperature anomaly patterns under each CT.

CT1+/CT1− present variations in the subtropical ridge south of South Africa. Under CT1+ the mid-latitude cyclone is relatively more enhanced at the south coast of southern Africa (Fig. 1). The associating wind pattern at the south coast of southern Africa under CT1+ is westerly (Fig. 4), and thickness anomaly is positive over South Africa except for the western tips, and also thickness anomaly is positive at the central parts of southern Africa except for large parts of Mozambique and Madagascar (Fig. 2a). Regions with positive thickness anomaly indicate warm advection and are generally associated with a positive temperature anomaly (Fig. 2b) as well as a negative relative humidity anomaly (Fig. 3).

Conversely, under CT1− the South Atlantic ridge is enhanced at the south coast of southern Africa, driving cold air, southeast into the southern African domain (Fig. 1 and Fig. 4), and also cyclonic activity is relatively more enhanced in the southwest Indian Ocean compared to CT1+. Given the cold air advection on the south coast of southern Africa, the thickness anomaly is negative over vast regions in South Africa (Fig. 2a). Under CT1−, the thickness anomaly is also negative over the central domains of southern Africa where the cold air from the South Atlantic high-pressure system advects, except for parts of Mozambique and Madagascar given the enhanced low-pressure system (that is, convective activity) over the oceans that results to warm air advection. Resultantly, regions with positive (negative) thickness anomaly values are generally characterized by positive (negative) temperature anomalies and negative (positive) relative humidity anomaly values (Fig. 2 and Fig. 3). The analysis of CT1+/CT1− indicates that cold advection resulting from circulation at the subtropical ridge implies lower thickness and lower temperature values in the regions where the cold air penetrates; similarly, enhancement of convective (or cyclonic activity) in the southwest Indian Ocean, results in warmer temperatures at the coastal landmasses.

Further, CT2+ presents circulation variability associated with enhancement of the anticyclonic circulation at the western branch of the Mascarene high and enhancement of the mid-latitude cyclone south of South Africa (Fig. 1). Hence the wind patterns are southeast over the southwest Indian Ocean, driven by the Mascarene high, and westerly, at the south coast of southern Africa (Fig. 4). Given that cold air advection from the South Atlantic anticyclone is weakened at the south coast of southern Africa, thickness anomaly is strongly positive at the south coast of southern Africa (Fig. 2a) as well as temperature anomaly (Fig. 2b). However, since the Mascarene high drives colder southeast winds into large parts of southern Africa, thickness anomaly is negative and temperature anomaly is negative over large parts of southern Africa. Resultantly, over the central parts of southern Africa, the pattern of CT2+ brings positive relative humidity anomaly, but negative relative humidity anomaly over parts of the southern tips that are anomalously warmer (Fig. 3). CT2 − is characterized by opposing (and asymmetric) circulation features, relative to CT2+, and so brings warmer (colder) temperatures over the central parts (southern tips) of southern Africa.

CT3+ is related to positive SAM and CT3 − is related to negative SAM (Ibebuchi 2021). We recall that the SAM through its control of circulation in the mid-latitudes significantly impacts the regions in southern Africa with the Mediterranean type of climate, that is, the Western Cape Province located in the southwestern part of southern Africa. Based on the climatology of the regions in southern Africa with the Mediterranean type of climate, the enhancement of the mid-latitude cyclones on the south coast of southern Africa under CT3 − (Fig. 1), and the associating westerly winds (Fig. 4) allow cold fronts to sweep across the southwestern parts of southern Africa. Thus, under CT3 − Figure 2a shows a zonal dipole-like structure of thickness anomaly whereby the eastern (western) region of South Africa has positive (negative) thickness anomaly values. As a result, temperature anomaly is positive (negative) in the eastern (western) region of South Africa (Fig. 2b). Also, the relative humidity anomaly is negative (positive) in the eastern (western) region of South Africa (Fig. 3) - an indication of a saturated atmosphere that eventually results in frontal rainfall in the western domain of South Africa. For the large parts in the central regions of southern Africa, Fig. 2 shows that under CT3− thickness and temperature anomalies are positive and relative humidity anomaly is equally negative (Fig. 3). The reason is that while CT3− is dominant in winter seasons (Fig. A1), nonetheless during its occurrence in DJF, SST and convergence are higher in the southwest Indian Ocean, and continental heating is equally higher compared to austral winter (JJA). Thus, during DJF, the displacement of atmospheric blocking by the western branch of the Mascarene high, and the resultant weakening of cold advection, allows warmer ocean waters in the southwest Indian Ocean (Vigaud et al., 2009). Hence, during the occurrence of CT3− in DJF, warm air advection from the southwest Indian Ocean, driven by the northeast trade winds (Fig. 4), leads to a warmer climate in large parts of southern Africa.

Further, CT3+ is associated with increased SLP in the mid-latitudes, but not the closed and elongated South Atlantic anticyclone that results in cold air advection from the Southern Ocean to large parts of South Africa (cf CT1− in Fig. 4). In this case (of CT3+), cold air advection to the eastern part of South Africa results from southeast winds driven by the western branch of the Mascarene high. Therefore, under CT3+ due to the cold air advection, the eastern part of South Africa has a negative thickness anomaly (Fig. 2a), negative temperature anomaly (Fig. 2b), and positive relative humidity anomaly (Fig. 3). Since westerly winds and the associating cold fronts are suppressed south of South Africa, the western region of South Africa has a positive thickness anomaly (Fig. 2a), positive temperature anomaly (Fig. 2b), and negative relative humidity anomaly (Fig. 3). For the central parts of southern Africa, due to the enhanced cold air advection by southeast winds driven by Mascarene high, negative thickness and temperature anomaly prevails over the central regions (Fig. 2) coupled with positive relative humidity anomaly (Fig. 3).

For the other CTs, similar patterns of variations in the pressure systems and the associating cold (warm) air advection, reduces (increase) the thickness of the air layer, resulting in negative (positive) temperature anomalies in preferred regions. For example, CT5− reinforces the findings from CT1− that when the South Atlantic Ocean high pressure is closed, ridging at the southern coast of southern Africa, large parts of South Africa become colder due to enhanced cold air advection (Fig. 1 to Fig. 4); and CT6+ depicts very similar pattern but with stronger amplitude. CT6− also reinforce previous findings that when southeast winds are enhanced by the circulation at the western branch of the Mascarene high then cold air advection to the eastern regions and large parts of southern Africa implies colder conditions in the study domain (Fig. 1 to Fig. 4).

CT7+/CT7− is related to the positive/negative SIOD (Ibebuchi, 2023). Under CT7+/CT7− the southwest Indian Ocean is warmer/cooler, based on the enhanced cyclonic/anticyclonic activity; in addition, the boundary layer in large parts of southern Africa is relatively unstable/stable under CT7+/CT7−. For CT7+, the pressure gradient between the South Atlantic high-pressure and the continental low results in cold air advection from the South Atlantic Ocean and the Southern Ocean to South Africa, but warm air advection from the (warmer) southwest Indian Ocean to the central regions of South Africa (Fig. 1, Fig. 2a and Fig. 4). Therefore, while colder temperatures are evident in the south and southwestern parts of South Africa, CT7+ brings warmer temperatures to the central domains of southern Africa (Fig. 2 to Fig. 3). Conversely, in CT7− cold advection from the southwest Indian Ocean prevails over the central parts of southern Africa (Fig. 2a and Fig. 4) and coupled with the stable atmosphere, leads to negative temperature anomalies over the central parts of southern Africa (Fig. 2b). But due to enhanced blocking of the mid-latitude cyclones at the southern coast of southern Africa, the activity of cold fronts that bring colder temperatures to the southwestern part of southern Africa is weakened so that the southwestern parts of southern Africa have positive temperature anomalies.

CT9− is remarkable and results in widespread positive temperature anomaly in South Africa (Fig. 2b). This is because of the meridional pressure gradient between the low pressure in the Mozambique Channel and the western branch of the Mascarene implying that colder southeast winds from the Mascarene high do not penetrate the eastern parts of South Africa (Fig. 1 and Fig. 4) coupled with the absence of the closed South Atlantic anticyclone at the southern coast of southern Africa. However, the pattern of CT9− also imply that colder air from the western branch of the Mascarene high move towards the low pressure in the Mozambique Channel, penetrating the central parts of South Africa and partly adjusting to westerly towards Madagascar (Fig. 4); this flow pattern brings negative thickness anomaly and colder temperatures to the central parts of southern Africa.

From Fig. A2, regions with a robust decrease in temperatures, for example, the western parts in CT3− and CT6+, and the eastern parts in CT7− (Fig. 2b), are mostly associated with low specific humidity; and regions with a robust increase in temperatures are mostly associated with high specific humidity, for example, the southeastern parts under CT3− and CT6+ and the southern parts under CT9−. This is generally because a warmer (colder) atmosphere can hold more (less) moisture. However, there are exceptions to this, for example under CT1−, where negative temperature anomaly at the southern parts of southern Africa is associated with positive specific humidity anomaly. This is because moisture content over the landmass is also modulated by other factors such as advection and moisture uptake over the oceans.

<u>Relationship between climatic modes and temperature variability over southern Africa</u>

Previous studies linked the CTs in Fig. 1 to climatic modes of variability. CT3+/CT3− was found to be modulated by the SAM (Ibebuchi 2021) such that CT3+ (CT3−) is related to positive (negative) SAM. CT5+/CT5 − was found to be modulated by the Nino 3.4 index (Ibebuchi 2022a), such that CT5 − (CT5+) is related to El Niño (La Niña). CT7+/CT7 − was found to be modulated by the SIOD (Ibebuchi 2023a), such that CT7+ (CT7 −) is related to the positive (negative) SIOD. CT9+/CT9 − was equally found to be modulated by the IOD (Ibebuchi 2023b) such that CT9+ (CT9 −) is related to the negative (positive) IOD. The frequency of these CTs is modulated by these large-scale modes of variability, and thus represent the regional-scale manifestations of the modes. That is the CTs are the physical mechanism through which these modes impact southern African temperatures.

In addition to the control of DJF temperatures by the climatic modes indirectly through the CTs, as shown in Figs 1 and 2, we also apply regression maps to examine the *direct* association between these well-known climatic modes and temperature in southern Africa. Figure 5 shows this association is spatially heterogeneous with a dipole structure especially over the southwestern and east-central parts of southern Africa. In terms of significant temperature increase, from Fig. 5, El Niño is associated with an increase in temperature over the central parts of southern Africa. The positive phase of the IOD is associated with an increase in temperature over the northeastern, northwestern and southwestern parts of southern Africa. The positive SAM is associated with temperature increase, mostly over the southwestern parts of southern Africa, while the SIOD is associated with temperature increase over the central/northcentral parts of southern Africa.

4 Discussion

The study by Liu et al. (2022) found that high-frequency atmospheric signals are crucial for improving sub-seasonal predictability of precipitation in most land monsoon regions. The high frequency intraseasonal variability was found to be responsible for a significant portion of the total intraseasonal variability and generally dominates the sub-seasonal predictability of various land monsoons. Liu et al. (2022) suggested that high frequency variability is necessary for enhancing predictability of climate variables such as precipitation and temperature at sub-seasonal time scales. The inclusion of high frequency variability in the CTs created in this work with the application of rotated T-mode PCA to daily SLP (Ibebuchi 2022a), in line with the recommendation of Liu et al. (2022), is necessary for the enhanced predictability of climate variables such as precipitation and temperature. This is because the multi-scale interaction between synoptic and inter-annual signals is connected by tropical and extratropical atmospheric signals affecting these CTs, on the intraseasonal time scales.

The majority of the studies linking atmospheric circulations to the climate of southern Africa are focused on precipitation (Barimalala et al., 2020; Fauchereau et al., 2009; Jury, 2015). Other studies have equally examined the relationship between climate drivers and precipitation variability in southern Africa (Hart et al., 2013; Hoell et al., 2015; Reason and Jagadheesha, 2005). Indeed, the studies concur that the hydroclimate of southern Africa is modulated by large-scale circulations. However, little attention has been given to the relationship between synoptic to large-scale circulations in southern Africa and temperature anomalies in southern African landmass. Among such studies, Gillet et al. (2006) investigated the relationship between the SAM and temperature in Southern Hemisphere landmasses. The authors found that positive SAM can be related to temperature increases over the southwestern parts of southern Africa, but temperature decreases over some northeastern parts. The results from Gillet et al. (2006) are consistent with the regression analysis between annual temperature anomalies and the SAM index in this study (Fig. 5). Also, the circulations through which positive SAM increases temperature of the southwestern parts of southern Africa (i.e., CT3+) is shown to be a poleward shift of westerly winds, which in turn suppresses the passage of cold fronts over the southwestern parts of southern Africa. The positive IOD increases SST over the tropical western Indian Ocean (Saji, 1999) and alters atmospheric circulations over southern Africa (Mantasa et al. 2011). Our results indicate that the SST pattern of the positive IOD is linked to temperature increase over Madagascar, the northeastern, northwestern and southwestern parts of southern Africa. Similarly, during El Niño and positive SIOD events, which are both associated with SST increase in the southwest Indian Ocean, temperature increase in some central parts of southern Africa can be expected. Also, El Niño and the positive SIOD appears to be related to temperature decreases over the southwestern parts of southern Africa possibly due to weakening of high-pressure adjacent to South Africa.

A previous study by Ibebuchi (2022b) investigated the effects of climate change on the atmospheric circulation types in southern Africa; it was found that under future climate change the frequency of occurrence, amplitude and spatial configuration of the classified CTs in this work are expected to change. Consequently, the relationship between atmospheric circulations over southern Africa and temperature variability will be impacted by climate change. As documented in Ibebuchi (2023), CMIP6 climate models projected summer periods of weaker circulation at the western branch of the Mascarene high due to warmer southwest Indian Ocean temperatures (i.e., CT4-) as well as summer periods of stronger circulation at the western branch of the Mascarene high due to a more positive SAM (i.e., CT3+). As shown in Figure 2a, a more positive SAM i.e., CT4+ (warmer southwest Indian Ocean i.e., CT3-) will imply warmer temperatures over the southwestern (southeastern) parts of southern Africa.

The climate of Southern Africa is influenced by a complex interplay of feedbacks between the atmosphere and surface processes. Changes in vegetation cover can impact the surface albedo, surface roughness, and evapotranspiration rates, which affect the temperature patterns in a region (e.g., Tran et al. 2017). For example, Clark and Arritt (1995) reported that vegetative cover can have a direct influence on increasing convective precipitation, by not only providing shade to reduce the conduction of heat into the soil (and thus increasing available heat energy in the atmosphere), but also via the extraction of soil moisture. Moreover, a study by Engelbrecht et al. (2015) used a regional climate model to project future temperature changes in Africa, finding that in (southern) Africa as temperature increases, the soils become drier through enhanced evaporation; and this, in turn, impacts vegetation.

Conclusions

This study investigated the mechanisms through which synoptic circulations control atmospheric layer thickness, temperature, relative and specific humidity in southern Africa, during the austral summer season. We also examined the impact of the SAM, IOD, ENSO and SIOD on temperatures in southern Africa. Our results on the synoptic circulations that modulate summer temperature in southern Africa can be summarized as follows:

1. The temperature in southern Africa exhibits spatial heterogeneity under the classified CTs. Thus, the distinct regional climate zones within the southern African landmass contribute to defining the spatial variations of temperature anomalies under a given CT.

2. Generally, two asymmetric variabilities in the semi-permanent high-pressure system influence regional temperature variations in southern Africa. First is when the South Atlantic Ocean high pressure is closed, and ridges at the southern coast of southern Africa; this synoptic circulation pattern is associated with the southeast wind to the southern parts of southern Africa from the ridging high pressure and causes cold air advection and negative temperature anomalies in the southern tip of southern Africa. Conversely, when the South Atlantic high is weak on the southern coast of southern Africa, westerly winds dominate over the southern coast of southern Africa, the thickness anomaly value is positive, and the temperature anomaly is positive in the southern parts of southern Africa. Second, when the anticyclonic circulation at the western branch of the Mascarene high is stronger, cold air advection by southeast winds is enhanced into large parts of southern Africa, reducing the atmospheric thickness layer and resulting in negative temperature anomalies. Conversely, when the anticyclonic circulation at the western branch of the Mascarene high is weak during the summer season, atmospheric blocking of the low-pressure system from the tropics is weakened as well, allowing enhanced cyclonic/convective activity in the southwest Indian Ocean; the implication is enhanced warm air advection into parts of southern Africa, increased thickness and positive temperature anomalies in parts of southern Africa. Hence when conditions are favorable, southeast winds from the semi-permanent high-pressure systems are mostly associated with colder temperatures in southern Africa.

3. Other variabilities that modulate summer temperature anomalies in southern Africa and interfere with circulations in the high-pressure systems are the formation of continental lows and the trough in the Mozambique Channel. Continental lows increase instability at the boundary layer, increase thickness, and summer temperature anomalies. Further, the strengthening of the Mozambique Channel trough coupled with a weak South

Atlantic anticyclone at the southern coast of southern Africa can be implicated to cause widespread warming over South Africa. This is because the aforementioned circulation pattern (i.e., CT9 −) increases the pressure gradient between Mascarene high and the low pressure in the Mozambique Channel so that cold air advection to South Africa is significantly limited.

4. Overall, at the synoptic scale, summer temperature anomalies in Madagascar are modulated by cold advection from the Mascarene high and warm advection resulting from a weaker Mascarene high and warmer southwest Indian Ocean waters.

5. Climate drivers such as SAM, ENSO, IOD and the SIOD impact temperatures over southern Africa. El Niño and positive SIOD are associated with temperature increase over the central parts of southern Africa. Positive SAM and positive IOD are associated with temperature increase over the southwestern parts of southern Africa, while additionally positive IOD is linked to temperature increase over the northwestern and northeastern parts of southern Africa.

Declarations

Conflict of interest: There are no conflicts of interest in this paper.

Funding statement: This research received no specific grant from any funding agency in the public, commercial, or not-for-profit sectors.

Author's Contribution: All authors worked together on all aspects of the manuscript

Availability of data and material: ERA5 data are available at https://cds.climate.copernicus.eu/cdsapp#!/dataset. The CPC data is available at https://psl.noaa.gov/data/gridded/data.cpc.globaltemp.html

Ethics approval: No human subject is involved in this study and Figures belong to the authors. The paper is also not under consideration in any Journal. There is also no conflict of interest in this paper

Consent to participate: No human research is used. The authors' consent for this paper to be considered

Consent for publication: The authors' consent for this paper to be published.

Reference

Alimonti, G., L. Mariani, F. Prodi, Ricci, R.A., 2022: A critical assessment of extreme events trends in times of global warming. Eur. Phys. J. Plus 137, 1–20.

Allen, M.J., Lee, C.C., 2014: Investigating high mortality during the cold season: mapping mean weather patterns of temperature and pressure. Theor. Appl. Climatol. 118, 419–428.

Barimalala, R., Blamey, R.C., Desbiolles, F., Reason, C.J., 2020: Variability in the Mozambique Channel Trough and impacts on southeast African rainfall. J. Clim. 33, 749–765.

Baudoin, M.-A., Vogel, C., Nortje, K., Naik, M., 2017: Living with drought in South Africa: lessons learnt from the recent El Niño drought period. Int. J. Disaster Risk Reduct. 23, 128–137.

Behera, S.K., Yamagata, T., 2001: Subtropical SST dipole events in the southern Indian Ocean. Geophys. Res. Lett. 28, 327–330.

Benjamini, Y. & Yekutieli, D. 2001: The control of the false discovery rate in multiple testing under dependency. Annals of statistics, 1165-1188.

Burls, N.J., Blamey, R.C., Cash, B.A., Swenson, E.T., Fahad, A. al, Bopape, M.-J.M., Straus, D.M., Reason, C.J., 2019: The Cape Town “Day Zero” drought and Hadley cell expansion. Npj Clim. Atmospheric Sci. 2, 1–8.

Clark, C. A., Arritt, P. W., 1995: Numerical simulations of the effect of soil moisture and vegetation cover on the development of deep convection. Journal of Applied Meteorology and Climatology, 34, 2029-2045.

Compagnucci, R.H., Richman, M.B., 2008: Can principal component analysis provide atmospheric circulation or teleconnection patterns? Int. J. Climatol. J. R. Meteorol. Soc. 28, 703–726.

Dieppois, B., Rouault, M., New, M., 2015: The impact of ENSO on Southern African rainfall in CMIP5 ocean atmosphere coupled climate models. Clim. Dyn. 45, 2425–2442.

Ding, Q., Steig, E.J., Battisti, D.S., Wallace, J.M., 2012: Influence of the tropics on the southern annular mode. J. Clim. 25, 6330–6348.

Engelbrecht, F., Adegoke, J., Bopape, M.J., Naidoo, M., Garland, R., Thatcher, M., McGregor, J., Katzfey, J., Werner, M., Ichoku, C. and Gatebe, C., 2015: Projections of rapidly rising surface temperatures over Africa under low mitigation. Environmental Research Letters, 10,p.085004.

Engelbrecht, C.J., Landman, W.A., 2016: Interannual variability of seasonal rainfall over the Cape south coast of South Africa and synoptic type association. Clim. Dyn. 47, 295–313.

Engelbrecht, C.J., Landman, W.A., Engelbrecht, F.A., Malherbe, J., 2015: A synoptic decomposition of rainfall over the Cape south coast of South Africa. Clim. Dyn. 44, 2589–2607.

Fauchereau, N., Pohl, B., Reason, C.J.C., Rouault, M., Richard, Y., 2009: Recurrent daily OLR patterns in the Southern Africa/Southwest Indian Ocean region, implications for South African rainfall and teleconnections. Clim. Dyn. 32, 575–591.

Flato, G., Marotzke, J., Abiodun, B., Braconnot, P., Chou, S.C., Collins, W., Cox, P., Driouech, F., Emori, S., Eyring, V., 2014: Evaluation of climate models, in: Climate Change 2013: The Physical Science Basis. Contribution of Working Group I to the Fifth Assessment Report of the Intergovernmental Panel on Climate Change. Cambridge University Press, pp. 741–866.

Gillett, N.P., Kell, T.D., Jones, P.D., 2006: Regional climate impacts of the Southern Annular Mode. Geophys. Res. Lett. 33.

Hart, N.C., Reason, C.J., Fauchereau, N., 2013: Cloud bands over southern Africa: Seasonality, contribution to rainfall variability and modulation by the MJO. Clim. Dyn. 41, 1199–1212.

Hendon, H.H., Thompson, D.W., Wheeler, M.C., 2007: Australian rainfall and surface temperature variations associated with the Southern Hemisphere annular mode. J. Clim. 20, 2452–2467.

Hersbach, H., Bell, B., Berrisford, P., Hirahara, S., Horányi, A., Muñoz-Sabater, J., Nicolas, J., Peubey, C., Radu, R., Schepers, D., 2020: The ERA5 global reanalysis. Q. J. R. Meteorol. Soc. 146, 1999–2049.

Hoell, A., Funk, C., Magadzire, T., Zinke, J., Husak, G., 2015: El Niño–Southern Oscillation diversity and southern Africa teleconnections during austral summer. Clim. Dyn. 45, 1583–1599.

Ibebuchi, C.C., 2021a: On the relationship between circulation patterns, the southern annular mode, and rainfall variability in Western Cape. Atmosphere 12, 753.

Ibebuchi, C.C., 2021b: Revisiting the 1992 severe drought episode in South Africa: the role of El Niño in the anomalies of atmospheric circulation types in Africa south of the equator. Theor. Appl. Climatol. 146, 723–740

Ibebuchi, C. C. 2022a. Circulation type analysis of regional hydrology: the added value in using CMIP6 over CMIP5 simulations as exemplified from the MPI-ESM-LR model. Journal of Water and Climate Change, 13(2), 1046-1055.

Ibebuchi, C. C., 2022b: Future trends in atmospheric circulation patterns over Africa south of the equator. Journal of Water and Climate Change, 13, 4194-4212.

Ibebuchi, C. C., 2022c: Can synoptic patterns influence the track and formation of tropical cyclones in the Mozambique Channel? AIMS Geosciences, 8,33-51

Ibebuchi, C.C., 2023a: Circulation patterns linked to the positive sub-tropical Indian Ocean dipole. Adv. Atmospheric Sci. 40, 110–128.

Ibebuchi, C.C., 2023b: Patterns of atmospheric circulation linking the positive tropical Indian Ocean dipole and southern African rainfall during summer. J Earth Syst Sci 132, 13

Jury, M.R., 2015: Passive suppression of South African rainfall by the Agulhas Current. Earth Interact. 19, 1–14.

Knittel, N., Jury, M.W., Bednar-Friedl, B., Bachner, G., Steiner, A.K., 2020: A global analysis of heat-related labour productivity losses under climate change—implications for Germany's foreign trade. Clim. Change 160, 251–269.

Lee, C.C., Sheridan, S.C., 2018: A new approach to modeling temperature-related mortality: Non-linear autoregressive models with exogenous input. Environ. Res. 164, 53–64.

Lee, C.C., Sheridan, S.C., Lin, S., 2012: Relating weather types to asthma-related hospital admissions in New York State. EcoHealth 9, 427–439.

Lennard, C., Hegerl, G., 2015: Relating changes in synoptic circulation to the surface rainfall response using self-organising maps. Clim. Dyn. 44, 861–879.

Liu, F., Wang, B., Ouyang, Y. et al. Intraseasonal variability of global land monsoon precipitation and its recent trend. npj Clim Atmos Sci 5, 30 (2022). https://doi.org/10.1038/s41612-022-00253-7

Lyon, B., Mason, S.J., 2007: The 1997–98 summer rainfall season in southern Africa. Part I: Observations. J. Clim. 20, 5134–5148.

Mahlalela, P.T., Blamey, R.C., Reason, C.J.C., 2019: Mechanisms behind early winter rainfall variability in the southwestern Cape, South Africa. Clim. Dyn. 53, 21–39.

Malherbe, J., Landman, W.A., Engelbrecht, F.A., 2014: The bi-decadal rainfall cycle, Southern Annular Mode and tropical cyclones over the Limpopo River Basin, southern Africa. Clim. Dyn. 42, 3121–3138.

Manatsa, D., Matarira C. H., Mukwada G. 2011: Relativeimpacts of ENSO and Indian Ocean dipole/zonal mode oneast SADC rainfall. Int J Climatol 31, 558–577. https://doi.org/10.1002/joc.2086

Manatsa, D., Mushore, T., Lenouo, A., 2017: Improved predictability of droughts over southern Africa using the standardized precipitation evapotranspiration index and ENSO. Theor. Appl. Climatol. 127, 259–274.

Morioka, Y., Takaya, K., Behera, S.K., Masumoto, Y., 2015: Local SST impacts on the summertime Mascarene high variability. J. Clim. 28, 678–694.

Pirhalla, D.E., Lee, C.C., Sheridan, S.C., Ransibrahmanakul, V., 2022: Atlantic coastal sea level variability and synoptic-scale meteorological forcing. J. Appl. Meteorol. Climatol. 61, 205–222.

Reason, C.J.C., 2001: Subtropical Indian Ocean SST dipole events and southern African rainfall. Geophys. Res. Lett. 28, 2225–2227.

Reason, C.J.C., Jagadheesha, D., 2005: A model investigation of recent ENSO impacts over southern Africa. Meteorol. Atmospheric Phys. 89, 181–205.

Reason, C.J.C., Rouault, M., 2005: Links between the Antarctic Oscillation and winter rainfall over western South Africa. Geophys. Res. Lett. 32.

Roffe, S. J., van der Walt, A. J. 2023: Representation and evaluation of southern Africa's seasonal mean and extreme temperatures in the ERA5-based reanalysis products. Atmospheric Research, 284, 106591.

Saji, N. H. et al., 1999: A dipole mode in the tropical Indian Ocean. Nature 401:360-363.

Sheridan, S.C., Allen, M.J., 2015: Changes in the frequency and intensity of extreme temperature events and human health concerns. Curr. Clim. Change Rep. 1, 155–162.

Sheridan, S.C., Dixon, P.G., 2017: Spatiotemporal trends in human vulnerability and adaptation to heat across the United States. Anthropocene 20, 61–73.

Sheridan, S.C., Lee, C.C., 2018: Temporal trends in absolute and relative extreme temperature events across North America. J. Geophys. Res. Atmospheres 123, 11,889-11,898.

Sheridan, S.C., Lee, C.C., Allen, M.J., 2019: The mortality response to absolute and relative temperature extremes. Int. J. Environ. Res. Public. Health 16, 1493.

Silvestri, G., Vera, C., 2009: Nonstationary impacts of the southern annular mode on Southern Hemisphere climate. J. Clim. 22, 6142–6148.

Tran, D. X., Pla, F., Latorre-Carmona, P., Myint, S. W., Caetano, M., Kieu, H. V., 2017: Characterizing the relationship between land use land cover change and land surface temperature. ISPRS Journal of Photogrammetry and Remote Sensing, 124, 119-132.

Vigaud, N., Richard, Y., Rouault, M., Fauchereau, N., 2009: Moisture transport between the South Atlantic Ocean and southern Africa: relationships with summer rainfall and associated dynamics. Clim. Dyn. 32, 113–123.

Wolski, P., Jack, C., Tadross, M., van Aardenne, L., Lennard, C., 2018: Interannual rainfall variability and SOM-based circulation classification. Clim. Dyn. 50, 479–492.

FIGURES

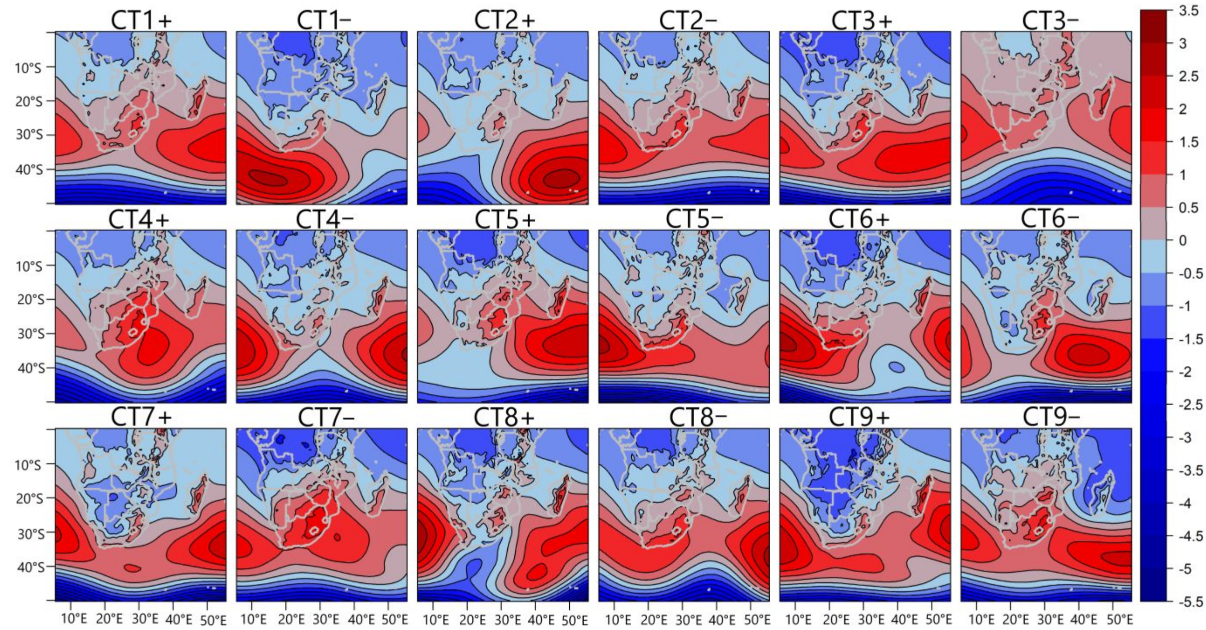

Fig. 1 z-score standardized SLP composite of the classified CTs

a)

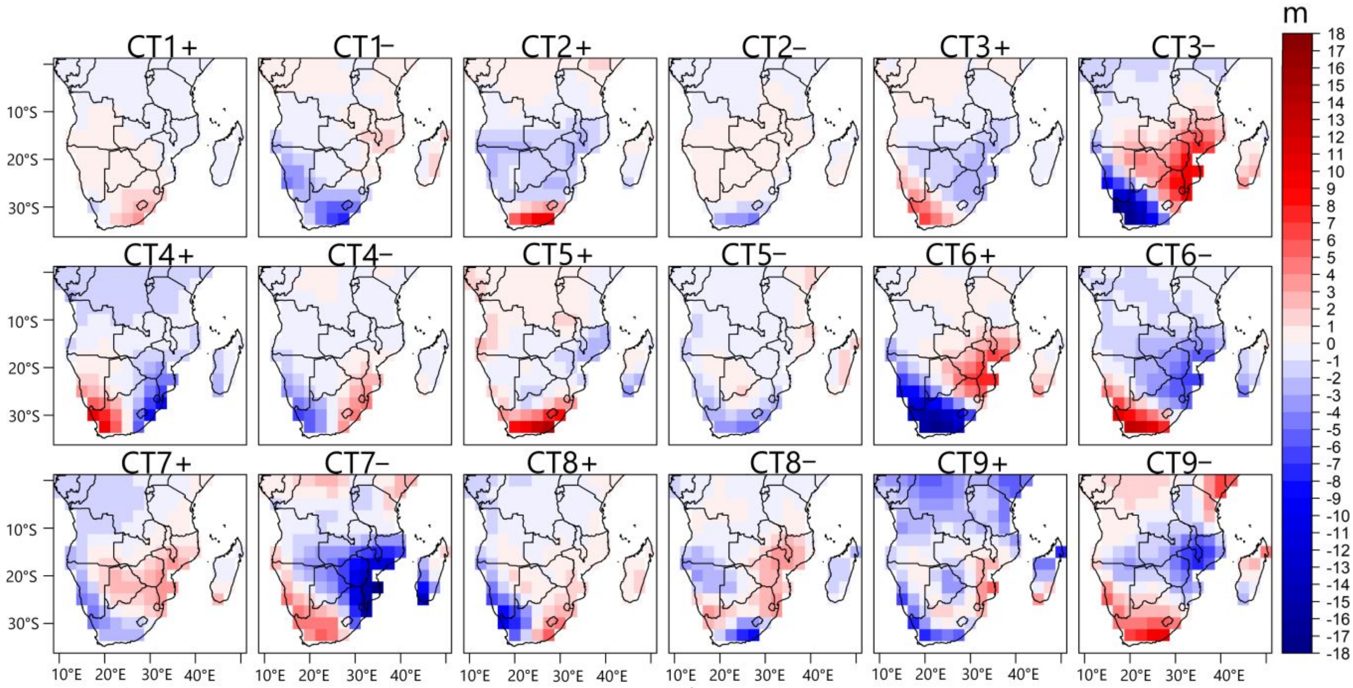

b)

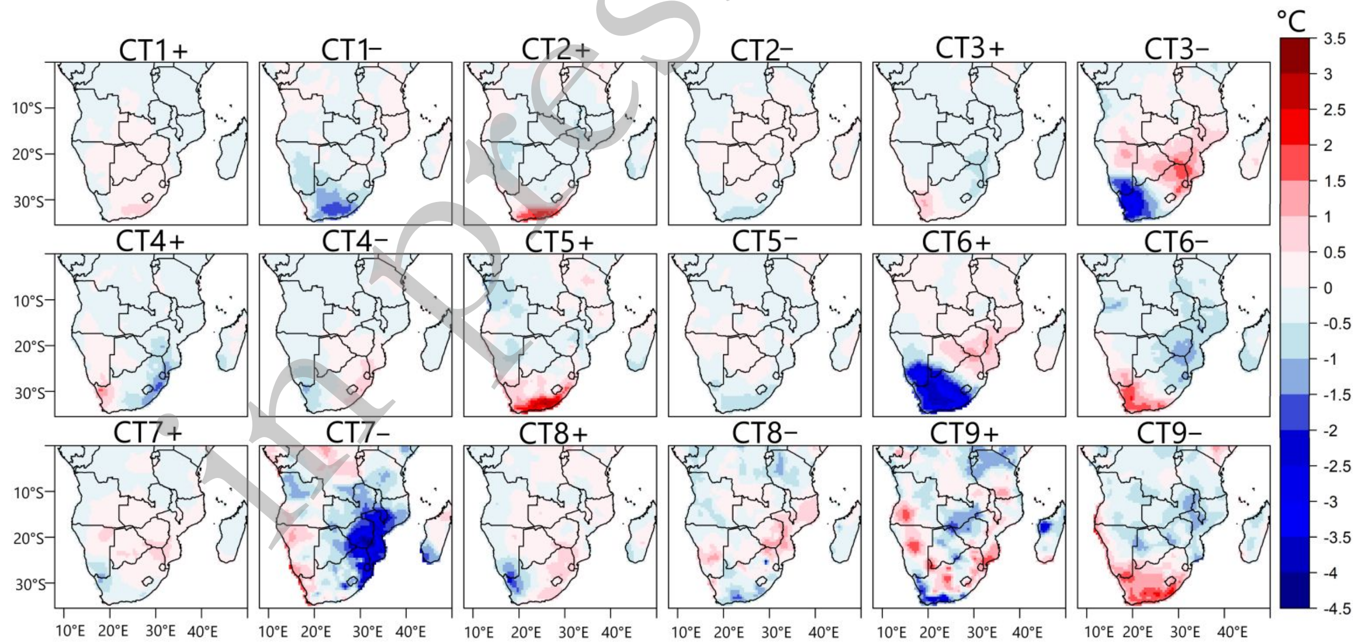

Fig. 2 Standardized composite anomaly maps of thickness layer between 1000 hPa and 850 hPa (a) and 2 m temperature anomaly during DJF for the classified CTs in Fig. 1

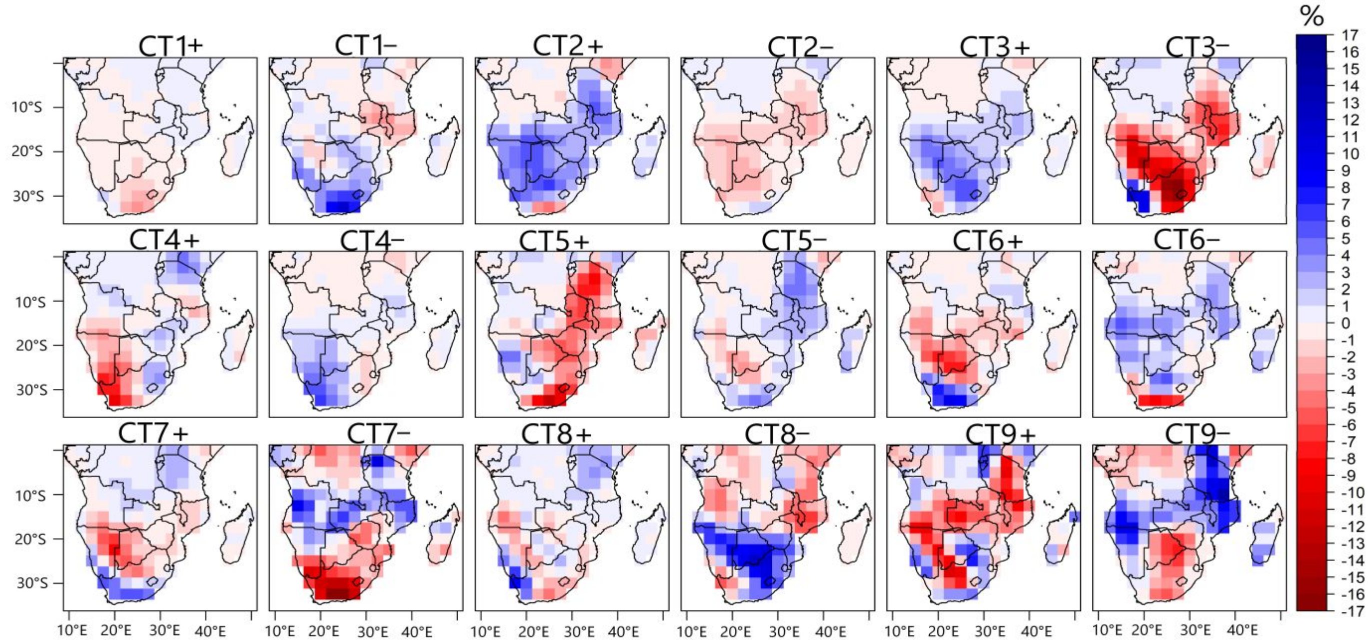

Fig. 3 Standardized composite anomaly maps of 850 hPa relative humidity during DJF for the classified CTs in Fig. 1

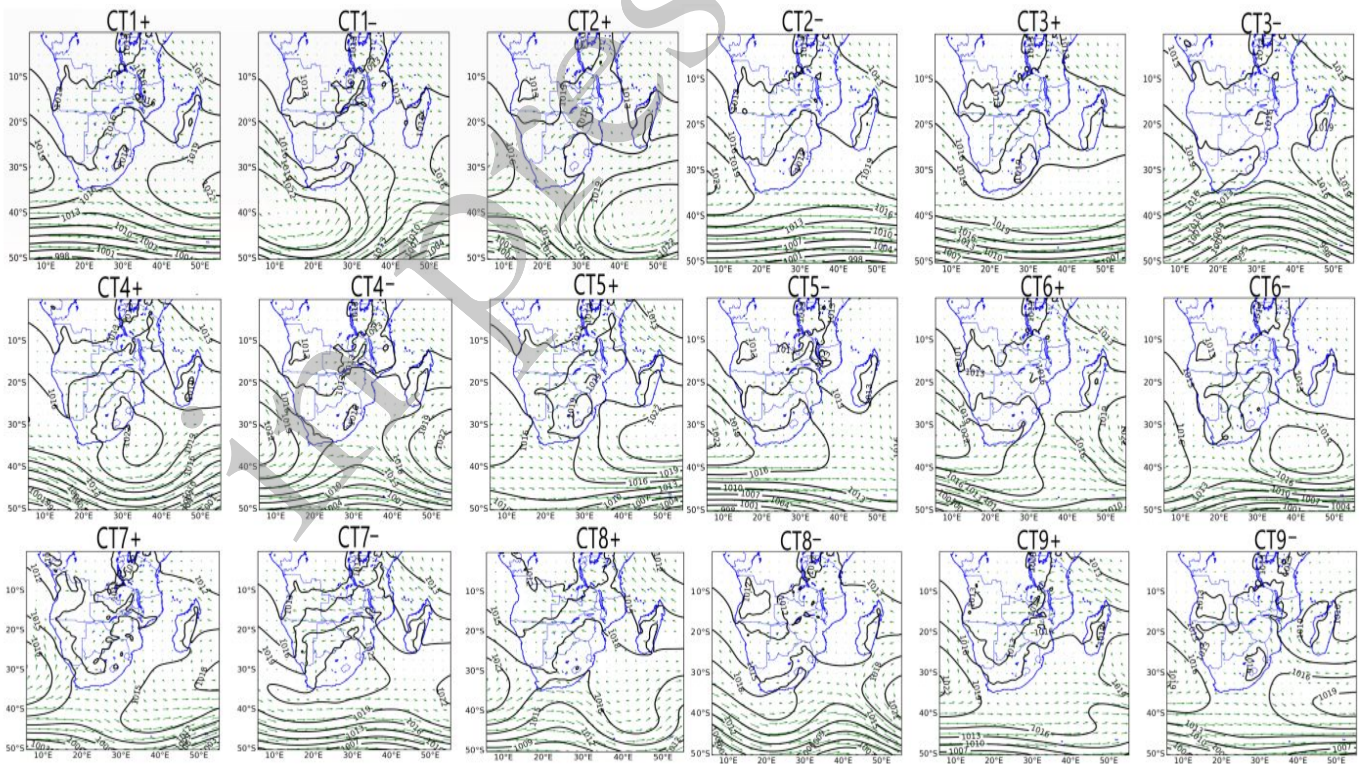

Fig. 4 Composite maps of SLP (black contours) and 850 hPa wind (green vectors) for the classified CTs in Fig. 1. The Contour interval is 3 hPa

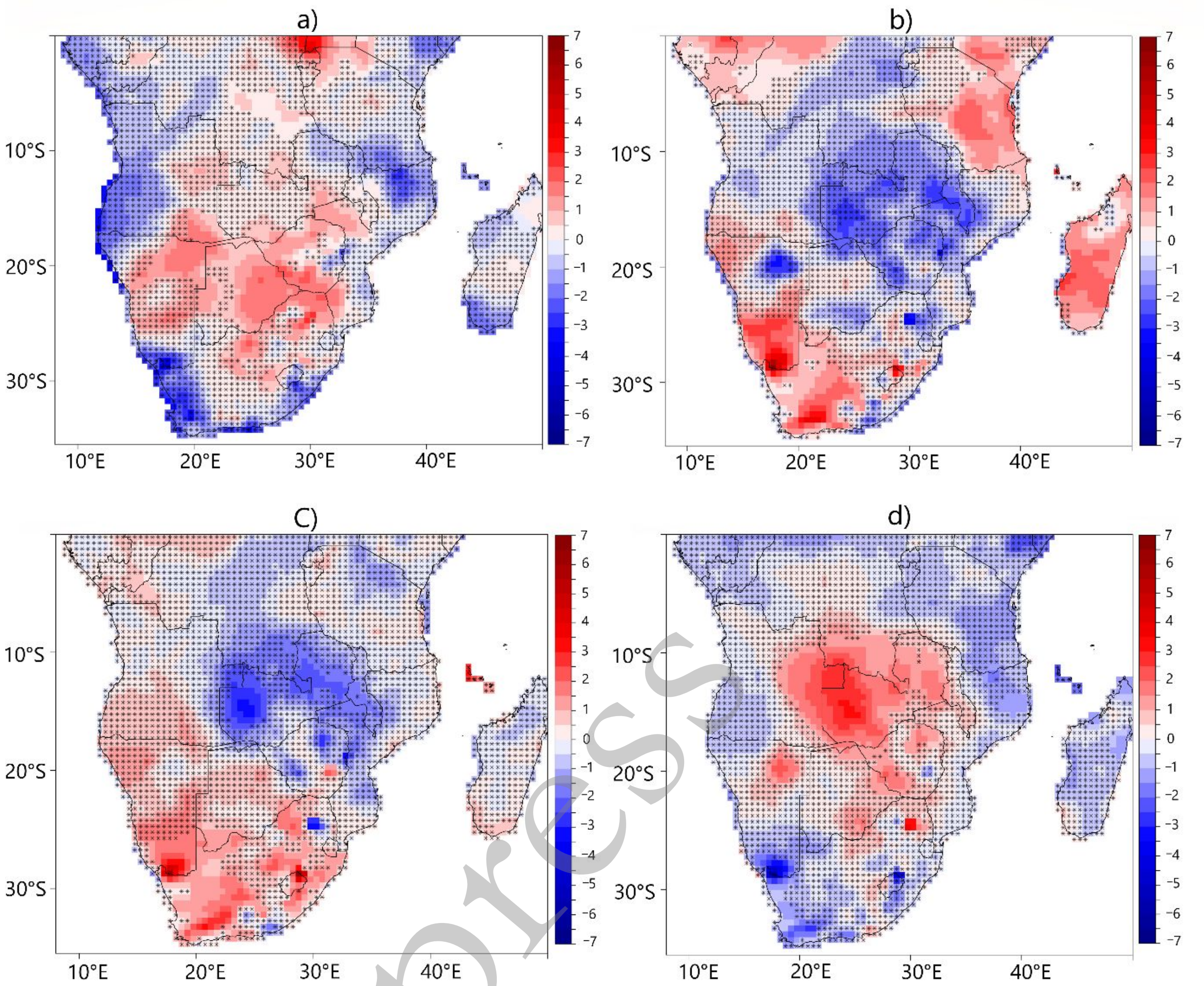

Fig. 5 Regression map of a) Nino 3.4 index; b) IOD index; c) SAM index; and d) SIOD index d) onto annual mean temperature anomaly in southern Africa from 1979 to 2021. Stippling shows grid points that are not statistically significant at a 95% confidence level.

Appendix A

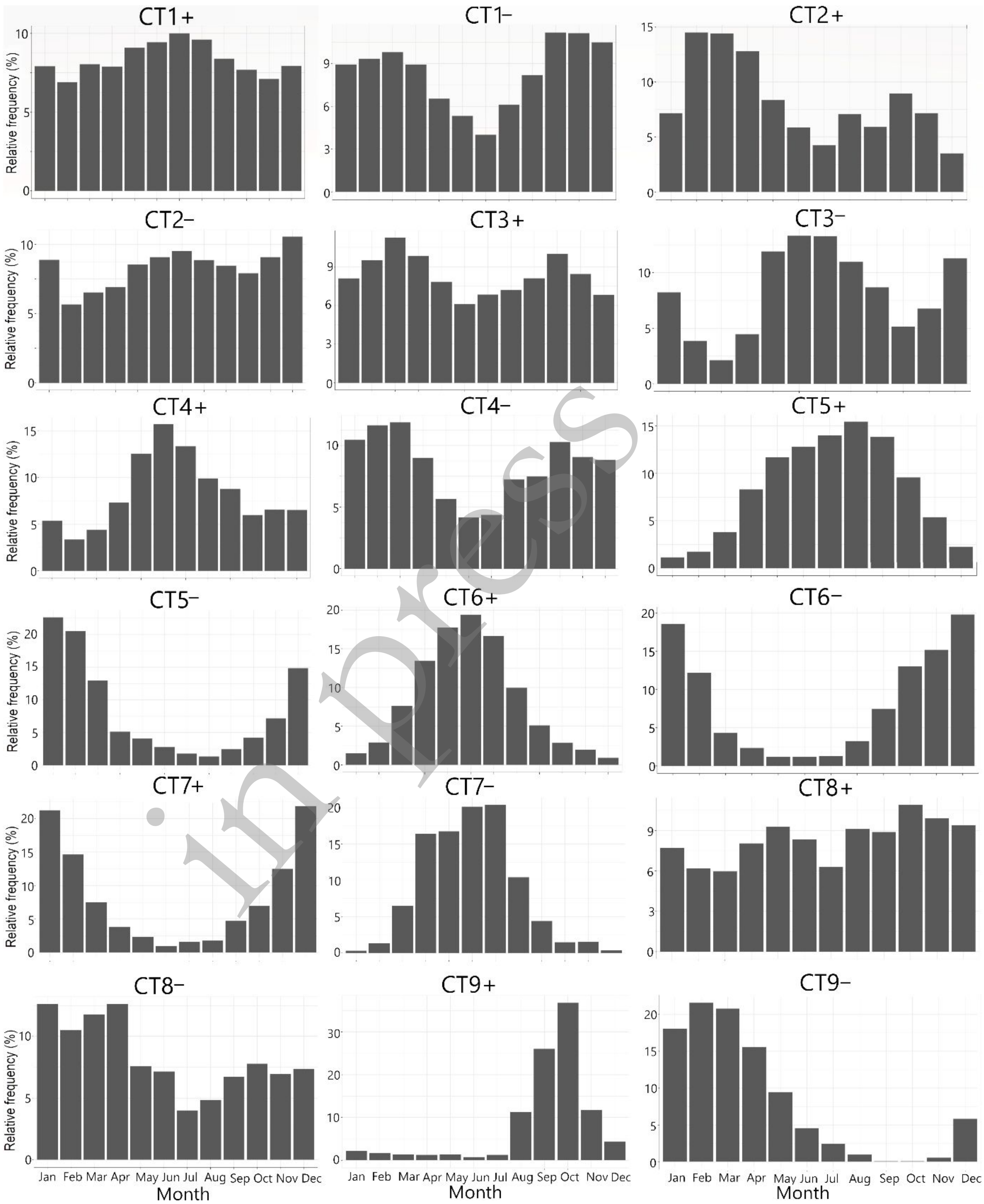
CT1+
CT1–
CT2+
CT2–
CT3+
CT3–
CT4+
CT4–
CT5+
CT5–
CT6+
CT6–
CT7+
CT7–
CT8+
CT8–
CT9+
CT9–
Relative frequency (%)
Jan Feb Mar Apr May Jun Jul Aug Sep Oct Nov Dec
Month

Fig. A1 Annual cycle of the CTs in Fig. 1. Y axis is the relative frequency of occurrence of the CTs and the x-axis is the calendar months.

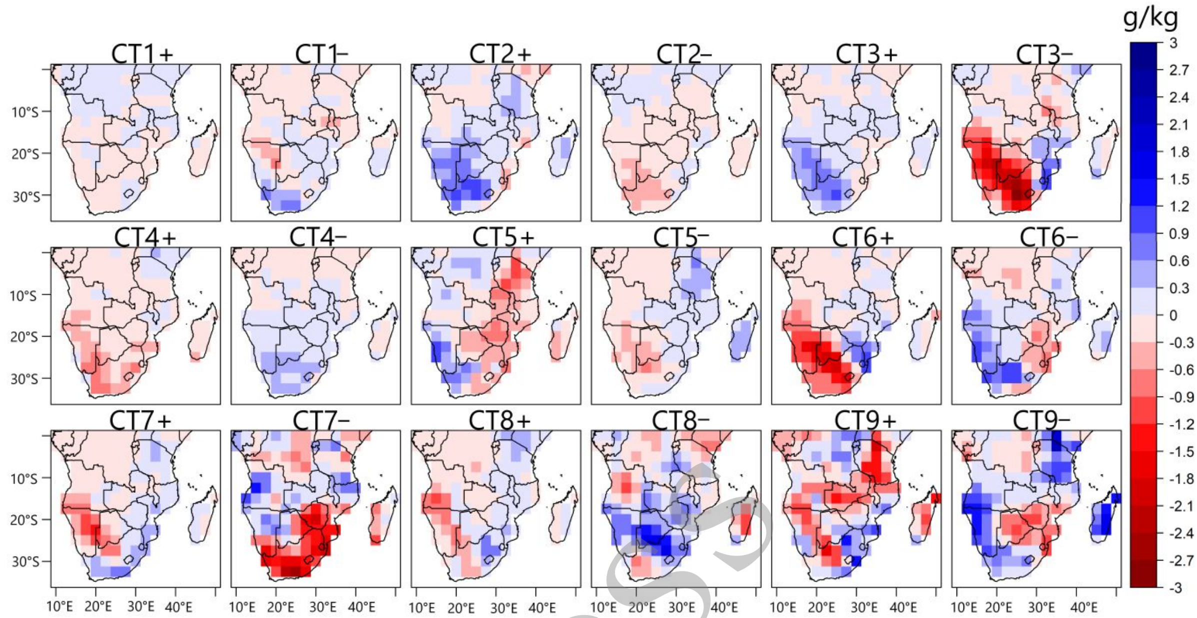

Fig. A2 Standardized composite anomaly maps of 850 hPa specific humidity during DJF for the CTs in Fig. 1

Classification of circulation types using the obliquely rotated T-mode PCA

The classification of the CTs is completely eigenvector-based (Richman 1981, 1986). It involves the application of obliquely rotated PCA to the T-mode matrix (variable or column matrix is time series and row matrix is grid points) of z-score standardized SLP field. The SLP field is standardized to give equal weight to all days in the analysis period. Singular value decomposition is applied to the correlation matrix, containing the correlation between SLP observations at each time in the analysis period, to obtain the PC scores, eigenvalues, and eigenvectors. The PC scores capture the spatial variability patterns, and the eigenvectors localize the spatial patterns in time. To make the eigenvectors responsive to rotation and to become correlations between the PC scores and the standardized SLP field, the eigenvectors are multiplied by the square root of their corresponding eigenvalues so that they become PC loadings that can be longer than a unit length. To enhance the physical interpretability of the PC loadings they were rotated obliquely using Promax at a power of 2. The oblique rotation simplifies the structure of the PCs by maximizing the number of near-zero loadings, so that unique time series with large loading magnitudes are clustered under a given PC. Given that we desire to analyse both dominant and (rare) patterns associated with extremes, of which the latter is often located in higher order PCs, we decide on the optimal number of PCs to retain and rotate by iteratively increasing the number of PCs until the next added PC is least unique from the already retained PCs. Since each PCs contains asymmetric patterns separated by the sign of the PC loadings, following its efficacy, in previous studies, ± 0.2 is used in this study to separate PC loadings in the signal range from PC loadings in the noise range. Introducing the threshold allows a day can be classified under more than one PC pattern insofar as the PC has signal magnitude >|0.2| on that day. Hence each retained PC gives two asymmetric classes (i.e., clusters above or below the ± 0.2 threshold) and the SLP mean of the days in a given class is the CT.

Circulation pattern controls of summer temperature anomalies in southern Africa

Chibuike Chiedozie Ibebuchi *[1,2], Cameron C. Lee[1,2]

[1] *Department of Geography, Kent State University, Kent, Ohio, USA*

[2] *ClimRISE Lab, Kent State University, Kent, Ohio, USA*

**Corresponding author's email:* cibebuch@kent.edu

Abstract

This study investigates the relationship between circulation patterns and austral summer temperature anomalies in southern Africa. The results show that the formation of continental lows tends to increase the partial atmospheric layer thickness. Further, the distinct variabilities of high and low pressure under the circulation types, influence air mass advection from the adjacent oceans, as well as atmospheric stability over land. Stronger anticyclonic circulation at the western branch of the Mascarene high enhances low-level cold air advection by southeast winds, decreases thickness, and lowers the temperature over a majority of the land in southern Africa. Conversely, a weaker Mascarene high, coupled with enhanced cyclonic activity in the southwest Indian Ocean increases low-level warm air advection and increases temperature anomalies over vast regions in southern Africa. The ridging of a closed South Atlantic anticyclone at the southern coast of southern Africa results in colder temperatures in the tip of southern Africa due to enhanced low-level cold air advection by southeast winds. However, when the ridge is weak and westerly winds dominate the southern coast of southern Africa, temperature increases in these areas. The northward track of the Southern Hemisphere mid-latitude cyclone, which can be linked to the negative Southern Annular Mode, reduces the temperature in the southwestern part of southern Africa. Also, during the analysis period, El Niño and the positive Subtropical Indian Ocean dipole were associated with temperature increases over the central parts of southern Africa; while the positive Indian Ocean dipole was linked to a temperature increase over the northeastern, northwestern, and southwestern parts of southern Africa.

Keywords: temperature, circulation types, Subtropical Indian Ocean dipole, Southern Annular Mode, El Niño, Indian Ocean dipole, Mascarene high, South Atlantic anticyclone

Highlights

- The spatiotemporal variations of temperature over southern Africa are coupled with large-scale circulation patterns modulating warm and cold air advection
- Climate drivers heterogeneously influence temperature over the land in southern Africa through control of regional circulation patterns.

1. Introduction

Rising global temperatures resulting from both anthropogenic emissions and natural variability impact virtually all aspects of livelihood, ranging from mortality rate (Lee and Sheridan, 2018; Sheridan and Dixon, 2017) and labor productivity (Knittel et al., 2020) to the rate and magnitude of climate extremes (Alimonti et al., 2022), among others. Climate predictions and projections are important for mitigating the consequences of rising temperatures by enhancing preparedness against extreme climate events as well as developing climate policies against future dangerous climate change. A major challenge in forecasting climate events, such as extreme temperatures, stems from the incomplete understanding of the physical mechanisms that drive the climate (Flato et al., 2014). Therefore, there is a need for studies that aim to improve the understanding of the atmospheric processes that govern the earth's climate. Enhanced knowledge of the atmospheric processes that govern the climate can serve as a benchmark for improving climate forecasts. In the regional context of southern Africa, which is vulnerable to anthropogenic climate change due to its economic conditions and geographical location at the descent region of the Hadley circulation (Baudoin et al., 2017), this study aims to enhance the understanding of the large scale circulations that modulate the summer temperatures in southern Africa.

Several studies have hinted at the role of climate drivers in modulating atmospheric circulations over southern Africa (Dieppois et al., 2015; Hoell et al., 2015; Lyon and Mason, 2007; Malherbe et al., 2014; Manatsa et al., 2017; Reason and Rouault, 2005) and other regions in the globe (Pirhalla et al., 2022). Among the climate drivers, the sea surface temperature (SST) patterns of the Subtropical Indian Ocean Dipole (SIOD) and the Southern Annular Mode (SAM) have a direct impact on the climate of southern Africa because they exist in the mid-latitude oceans of the Southern hemisphere (i.e., the subtropical Indian Ocean, and the Southern Ocean). In addition, the Indian Ocean Dipole (IOD) and the El Niño Southern Oscillation (ENSO) have a remote influence on the climate of southern Africa (Reason and Jagadheesha, 2005). Moreover, the imprint of the ENSO signal can be found in the SAM, IOD and SIOD modes since all the climate drivers generally influence SST anomalies in the southwest Indian Ocean as well as the anticyclonic circulation of the Mascarene high. (Ding et al., 2012; Ibebuchi, 2021; Morioka et al., 2015). Therefore, this study also investigates the impact of the climate drivers on temperature variability in southern Africa.

The link between synoptic circulations and precipitation in southern Africa has been widely documented (Burls et al., 2019; Engelbrecht et al., 2015; Engelbrecht and Landman, 2016; Lennard and Hegerl, 2015; Mahlalela et al., 2019; Wolski et al., 2018). Also, studies have highlighted the possible impact of the SAM on temperature anomalies in southern Africa. For example, using regression analysis, (Gillett et al., 2006) investigated the impact of positive

SAM on temperatures in the Southern Hemisphere (with the inclusion of southern Africa), however, the negative SAM was not considered and the associating physical processes were not analyzed in detail. Also for other regions in the Southern Hemisphere, such as Australia and South America, studies have addressed the relationship between the SAM and surface temperatures (Hendon et al., 2007; Silvestri and Vera, 2009). Further, the majority of available works of literature on the IOD and SIOD, with regard to the climate of southern Africa, focus on the relationship between the climate drivers and rainfall variability in southern Africa (Behera and Yamagata, 2001; Hoell et al., 2015; Ibebuchi, 2023; Reason, 2001), and less attention is given to temperature. Given that these climate drivers impact the amplitude and frequency of circulation types (CTs), this study goes further to decompose in time, the distinct circulations in southern Africa and then analyze the mechanisms through which the individual CTs impact surface temperature and relative humidity (that contributes to heat stress) in southern Africa. Thus, the major added value of this study to the literature is the improved understanding of the physical processes through which large-scale circulations influence the spatial variations and magnitude of summer temperatures in southern Africa.

This study is structured as follows, Section 2 presents the data and methods the study is based on; the results are presented in Section 3; Section 4 contains the discussion of the results and conclusions.

2 Data and methodology

2.1 Data

High-resolution reanalysis data is obtained from ERA5 (Hersbach et al., 2020). The ERA5 reanalysis data sets obtained are sea level pressure (SLP); 850 hPa wind vectors, relative humidity, specific humidity, 850 hPa geopotential height; and 1000 hPa geopotential height. Gridded observed 2 m average temperature is obtained from the Climate Prediction Center (CPC) Global Unified Temperature dataset (https://psl.noaa.gov/data/gridded/data.cpc.globaltemp.html). All data sets are obtained at daily temporal resolution from 1979 to 2021. The horizontal resolution of the ERA5 reanalysis data is 0.25° longitude and latitude, and 0.5° longitude and latitude for the gridded CPC 2 m temperature data. Also, correspondence between ERA5 and gridded CPC temperature data has been reported (Roffe and van der Walt 2023), which strengthens the choice of using both data sets for our analysis.

2.2 Methodology

This current study is incremental work from previous research that applied circulation typing to study circulations in southern Africa at multiple spatial scales (Ibebuchi, 2023a), hence the same classified CTs are used. A major advancement in this study is that these same CTs are now being used to investigate the mechanisms through which circulation patterns modulate the magnitude and spatial variations of austral summer (i.e., December to February – DJF) *temperature* in southern Africa. We consider austral summer as that is when absolute temperatures are highest in the study region, and thus, most impactful. The spatial extent for the CT classification is 0° to 50.25°S and 5.25°E to 55.25°E (Fig. 1). The adjacent maritime regions that act as moisture sources to the landmass were included. Further, when the CTs are linked to temperature over the landmass, typically, to make a distinction with the tropical landmass, southern Africa might be defined to include landmass from about 10°S and poleward.

Nonetheless, we have included the tropical latitudes (i.e., up to 0° latitude) to capture variability in the cross-equatorial northeast trade winds. This is because the cross-equatorial northeast trade winds play a role in defining convergence in the Angola Low and the Mozambique Channel that both impact the climate of southern Africa. However, we focus our analysis on the temperature anomalies under the distinct CTs on land from 10°S and poleward.

The obliquely rotated T-mode (variable is time series and observation is grid points) principal component analysis (Compagnucci and Richman, 2008) applied in a fuzzy approach is used for the classification of the CTs. The details of the classification approach are given in Appendix A. The classification of the CTs with rotated T-mode PCA is a time decomposition technique. Singular value decomposition is applied to the correlation matrix containing the correlation between the SLP fields at the distinct daily time series in the analysis period. The resulting PC loadings which designate the amplitude of the set of circulation patterns at a given day is used to assign CT(s) within the signal range to a given day, which imply the CTs that occurred on the day in question.

We apply map composting of different climate variables to examine the relationship between the classified CTs and DJF temperatures in southern Africa. We have used SLP composites to investigate the horizontal variations of pressure under each of the CTs, which can also be suitable for characterizing continental heating (i.e., in areas with continental lows) as well as atmospheric stability at the boundary layer, and convective activity over the adjacent oceans. We defined the thickness of the atmospheric layer as the vertical distance in meters between two the 1000 hPa and 850 hPa pressure levels. This is because, we found that from iterative pre-evaluations, relatively, the thickness layer values between 1000 hPa and 850 hPa accurately capture the spatiotemporal variations of 2 m mean temperature values in the study region. Thus, we define thickness as the difference between the height at 850 hPa and the height at 1000 hPa.

Positive thickness values are related to positive temperature anomalies and negative thickness values are related to negative temperature anomalies. In addition to analyzing the SLP and atmospheric layer thickness, composites of 850 hPa (that is, the height above the eastern escarpment of southern Africa) winds are analyzed to establish the prevailing winds under each CT. Thus, analyzing the SLP, wind directions, and thickness enables documenting low-level cold and warm air advection under each CT.

Given the high seasonality of temperature, to enable a robust diagnosis of the temperature values and other variables used to diagnose temperature patterns under each CT, we rely on composite anomaly values during DJF. The composite anomaly is calculated as the difference between the days assigned to a CT and the 1981-2010 DJF climatology of the variable in question. Regression analysis was used to investigate, at each grid point in the region of assessment, the association between climate drivers (SAM, ENSO, IOD and SIOD) and temperature variability in southern Africa. The statistical significance of the association, based on the regression model, is tested at a 95% confidence level. To control for false discovery rate in the multiple hypothesis testing, we used the Benjamini-Hochberg procedure (Benjamini, and Yekutieli, 2001), which assumes that the hypotheses being tested are independent.

3 Results

The standardized SLP composites for the days when the classified CTs occurred during the analysis period are shown in Figure 1. The CTs in Figure 1 were externally validated using SLP data from a different reanalysis product (Ibebuchi 2022c) and a suite of CMIP6 general circulation models (Ibebuchi 2022b). While the CTs are not confined to occur in any specific season, the spatiotemporal structure and dynamics of the CTs can also be influenced by seasonal variations in large-scale processes such as diabatic heating, thus the CTs tend to be dominant in specific seasons when the prevailing (seasonal) atmospheric condition favors their mechanisms (Fig. A1). Pressure variations over the adjacent oceans are used to infer convective activity in these locations – anticyclonic (cyclonic) circulations over the oceans imply suppressed (enhanced) convection. Similarly, pressure variations over the landmass can be used to infer continental heating or atmospheric stability at the boundary layer – anticyclonic (cyclonic) circulations over the land imply a relatively stable (unstable) atmosphere.

Next, for the classified CTs in Fig. 1, we look at the composite anomaly patterns of DJF atmospheric layer thickness between 1000 hPa to 850 hPa (Fig. 2a), temperature (Fig. 2b), and 850 hPa relative humidity (Fig. 3); and composite patterns of 850 hPa wind vectors (Fig. 4). These figures will be interpreted coherently, based on the asymmetric patterns of the CTs (i.e., the positive phase and the negative phase). We focus our analysis of the composite anomaly maps in Figs 2 to 3 mostly on the regions (i.e., group of grid points) with robust changes.

Generally, the composite patterns reveal that under each CT, the DJF temperature anomalies are characterized by spatial heterogeneity (Fig. 2b). A possible explanation for the spatial heterogeneity of temperature anomalies under each CT can be due to the distinct regional climates in southern Africa. Under the asymmetry of each CT (i.e., the negative and positive phases) temperature variations are least in the deep tropics (10°S – 0°) mostly because, diabatic heating (and SLP) have fewer variations in the deep tropics. However, as noted earlier, the major focus of the temperature anomalies is on southern Africa. Fig. 2a indicates that for the asymmetry of a given CT, and depending on the circulation features, there appear to be coherent temperature patterns in the central parts of southern Africa – mostly at landmasses close to the southwest Indian Ocean - at the southwestern parts of southern Africa, characterized by the Mediterranean type of climate, and at the southern tip of southern Africa. Thus, the regional climate types of the aforementioned regions contribute to defining the overall spatial heterogeneity of the temperature anomaly patterns under each CT.

CT1+/CT1− present variations in the subtropical ridge south of South Africa. Under CT1+ the mid-latitude cyclone is relatively more enhanced at the south coast of southern Africa (Fig. 1). The associating wind pattern at the south coast of southern Africa under CT1+ is westerly (Fig. 4), and thickness anomaly is positive over South Africa except for the western tips, and also thickness anomaly is positive at the central parts of southern Africa except for large parts of Mozambique and Madagascar (Fig. 2a). Regions with positive thickness anomaly indicate warm advection and are generally associated with a positive temperature anomaly (Fig. 2b) as well as a negative relative humidity anomaly (Fig. 3).

Conversely, under CT1− the South Atlantic ridge is enhanced at the south coast of southern Africa, driving cold air, southeast into the southern African domain (Fig. 1 and Fig. 4), and cyclonic activity is relatively more enhanced in the southwest Indian Ocean compared to CT1+. Given the cold air advection on the south coast of southern Africa, the thickness anomaly is negative over vast regions in South Africa (Fig. 2a). Under CT1−, the thickness anomaly is also negative over the central domains of southern Africa where the cold air from the South Atlantic high-pressure system advects, except for parts of Mozambique and Madagascar given the enhanced low-pressure system (that is, convective activity) over the oceans that results to warm air advection. Resultantly, regions with positive (negative) thickness anomaly values are generally characterized by positive (negative) temperature anomalies and negative (positive) relative humidity anomaly values (Fig. 2 and Fig. 3). The analysis of CT1+/CT1− indicates that cold advection resulting from circulation at the subtropical ridge implies lower thickness and lower temperature values in the regions where the cold air penetrates; similarly, enhancement of convective (or cyclonic activity) in the southwest Indian Ocean, results in warmer temperatures at the coastal landmasses.

Further, CT2+ presents circulation variability associated with enhancement of the anticyclonic circulation at the western branch of the Mascarene high and enhancement of the mid-latitude cyclone south of South Africa (Fig. 1). Hence the wind patterns are southeast over the southwest Indian Ocean, driven by the Mascarene high, and westerly, at the south coast of southern Africa (Fig. 4). Given that cold air advection from the South Atlantic anticyclone is weakened at the south coast of southern Africa, thickness anomaly is strongly positive at the south coast of southern Africa (Fig. 2a) as well as temperature anomaly (Fig. 2b). However, since the Mascarene high drives colder southeast winds into large parts of southern Africa, thickness anomaly is negative and temperature anomaly is negative over large parts of southern Africa. Resultantly, over the central parts of southern Africa, the pattern of CT2+ brings positive relative humidity anomaly, but negative relative humidity anomaly over parts of the southern tips that are anomalously warmer (Fig. 3). CT2 − is characterized by opposing (and asymmetric) circulation features, relative to CT2+, and so brings warmer (colder) temperatures over the central parts (southern tips) of southern Africa.

CT3+ is related to positive SAM and CT3 − is related to negative SAM (Ibebuchi 2021). We recall that the SAM through its control of circulation in the mid-latitudes significantly impacts the regions in southern Africa with the Mediterranean type of climate, that is, the Western Cape Province located in the southwestern part of southern Africa. Based on the climatology of the regions in southern Africa with the Mediterranean type of climate, the enhancement of the mid-latitude cyclones on the south coast of southern Africa under CT3 − (Fig. 1), and the associating westerly winds (Fig. 4) allow cold fronts to sweep across the southwestern parts of southern Africa. Thus, under CT3 − Figure 2a shows a zonal dipole-like structure of thickness anomaly whereby the eastern (western) region of South Africa has positive (negative) thickness anomaly values. As a result, temperature anomaly is positive (negative) in the eastern (western) region of South Africa (Fig. 2b). Also, the relative humidity anomaly is negative (positive) in the eastern (western) region of South Africa (Fig. 3) - an indication of a saturated atmosphere that eventually results in frontal rainfall in the western domain of South Africa. For the large parts in the central regions of southern Africa, Fig. 2 shows that under CT3− thickness and temperature anomalies are positive and relative humidity anomaly is equally negative (Fig. 3). The reason is that while CT3− is dominant in winter seasons (Fig. A1), nonetheless during its occurrence in DJF, SST and convergence are higher in the southwest Indian Ocean, and continental heating is equally higher compared to austral winter (JJA). Thus, during DJF, the displacement of atmospheric blocking by the western branch of the Mascarene high, and the resultant weakening of cold advection, allows warmer ocean waters in the southwest Indian Ocean (Vigaud et al., 2009). Hence, during the occurrence of CT3− in DJF, warm air advection from the southwest Indian Ocean, driven by the northeast trade winds (Fig. 4), leads to a warmer climate in large parts of southern Africa.

Further, CT3+ is associated with increased SLP in the mid-latitudes, but not the closed and elongated South Atlantic anticyclone that results in cold air advection from the Southern Ocean to large parts of South Africa (cf CT1− in Fig. 4). In this case (of CT3+), cold air advection to the eastern part of South Africa results from southeast winds driven by the western branch of the Mascarene high. Therefore, under CT3+ due to the cold air advection, the eastern part of South Africa has a negative thickness anomaly (Fig. 2a), negative temperature anomaly (Fig. 2b), and positive relative humidity anomaly (Fig. 3). Since westerly winds and the associating cold fronts are suppressed south of South Africa, the western region of South Africa has a positive thickness anomaly (Fig. 2a), positive temperature anomaly (Fig. 2b), and negative relative humidity anomaly (Fig. 3). For the central parts of southern Africa, due to the enhanced cold air advection by southeast winds driven by Mascarene high, negative thickness and temperature anomaly prevails over the central regions (Fig. 2) coupled with positive relative humidity anomaly (Fig. 3).

For the other CTs, similar patterns of variations in the pressure systems and the associating cold (warm) air advection, reduces (increase) the thickness of the air layer, resulting in negative (positive) temperature anomalies in preferred regions. For example, CT5− reinforces the findings from CT1− that when the South Atlantic Ocean high pressure is closed, ridging at the southern coast of southern Africa, large parts of South Africa become colder due to enhanced cold air advection (Fig. 1 to Fig. 4); and CT6+ depicts very similar pattern but with stronger amplitude. CT6− also reinforce previous findings that when southeast winds are enhanced by the circulation at the western branch of the Mascarene high then cold air advection to the eastern regions and large parts of southern Africa implies colder conditions in the study domain (Fig. 1 to Fig. 4).

CT7+/CT7− is related to the positive/negative SIOD (Ibebuchi, 2023). Under CT7+/CT7− the southwest Indian Ocean is warmer/cooler, based on the enhanced cyclonic/anticyclonic activity; in addition, the boundary layer in large parts of southern Africa is relatively unstable/stable under CT7+/CT7−. For CT7+, the pressure gradient between the South Atlantic high-pressure and the continental low results in cold air advection from the South Atlantic Ocean and the Southern Ocean to South Africa, but warm air advection from the (warmer) southwest Indian Ocean to the central regions of South Africa (Fig. 1, Fig. 2a and Fig. 4). Therefore, while colder temperatures are evident in the south and southwestern parts of South Africa, CT7+ brings warmer temperatures to the central domains of southern Africa (Fig. 2 to Fig. 3). Conversely, in CT7− cold advection from the southwest Indian Ocean prevails over the central parts of southern Africa (Fig. 2a and Fig. 4) and coupled with the stable atmosphere, leads to negative temperature anomalies over the central parts of southern Africa (Fig. 2b). But due to enhanced blocking of the mid-latitude cyclones at the southern coast of southern Africa, the activity of cold fronts that bring colder temperatures to the southwestern part of southern Africa is weakened so that the southwestern parts of southern Africa have positive temperature anomalies.

CT9− is remarkable and results in widespread positive temperature anomaly in South Africa (Fig. 2b). This is because of the meridional pressure gradient between the low pressure in the Mozambique Channel and the western branch of the Mascarene implying that colder southeast winds from the Mascarene high do not penetrate the eastern parts of South Africa (Fig. 1 and Fig. 4) coupled with the absence of the closed South Atlantic anticyclone at the southern coast of southern Africa. However, the pattern of CT9− also imply that colder air from the western branch of the Mascarene high move towards the low pressure in the Mozambique Channel, penetrating the central parts of South Africa and partly adjusting to westerly towards Madagascar (Fig. 4); this flow pattern brings negative thickness anomaly and colder temperatures to the central parts of southern Africa.

From Fig. A2, regions with a robust decrease in temperatures, for example, the western parts in CT3− and CT6+, and the eastern parts in CT7− (Fig. 2b), are mostly associated with low specific humidity; and regions with a robust increase in temperatures are mostly associated with high specific humidity, for example, the southeastern parts under CT3− and CT6+ and the southern parts under CT9−. This is generally because a warmer (colder) atmosphere can hold more (less) moisture. However, there are exceptions to this, for example under CT1−, where negative temperature anomaly at the southern parts of southern Africa is associated with positive specific humidity anomaly. This is because moisture content over the landmass is also modulated by other factors such as advection and moisture uptake over the oceans.

Relationship between climatic modes and temperature variability over southern Africa

Previous studies linked the CTs in Fig. 1 to climatic modes of variability. CT3+/CT3− was found to be modulated by the SAM (Ibebuchi 2021a) such that CT3+ (CT3−) is related to positive (negative) SAM. CT5+/CT5− was found to be modulated by the Nino 3.4 index (Ibebuchi 2021b), such that CT5− (CT5+) is related to El Niño (La Niña). CT7+/CT7− was found to be modulated by the SIOD (Ibebuchi 2023a), such that CT7+ (CT7−) is related to the positive (negative) SIOD. CT9+/CT9− was equally found to be modulated by the IOD (Ibebuchi 2023b) such that CT9+ (CT9−) is related to the negative (positive) IOD. The frequency of these CTs is modulated by these large-scale modes of variability, and thus represent the regional-scale manifestations of the modes. That is the CTs are the physical mechanism through which these modes impact southern African temperatures.

In addition to the control of DJF temperatures by the climatic modes indirectly through the CTs, as shown in Figs 1 and 2, we also apply regression maps to examine the *direct* association between these well-known climatic modes and temperature in southern Africa. Figure 5 shows this association is spatially heterogeneous with a dipole structure especially over the southwestern and east-central parts of southern Africa. In terms of significant temperature increase, from Fig. 5, El Niño is associated with an increase in temperature over the central parts of southern Africa. The positive phase of the IOD is associated with an increase in temperature over the northeastern, northwestern and southwestern parts of southern Africa. The positive SAM is associated with temperature increase, mostly over the southwestern parts of southern Africa, while the SIOD is associated with temperature increase over the central/northcentral parts of southern Africa.

4 Discussion

The study by Liu et al. (2022) found that high-frequency atmospheric signals are crucial for improving sub-seasonal predictability of precipitation in most land monsoon regions. The high frequency intraseasonal variability was found to be responsible for a significant portion of the total intraseasonal variability and generally dominates the sub-seasonal predictability of various land monsoons. Liu et al. (2022) suggested that high frequency variability is necessary for enhancing predictability of climate variables such as precipitation and temperature at sub-seasonal time scales. The inclusion of high frequency variability in the CTs created in this work with the application of rotated T-mode PCA to daily SLP (Ibebuchi 2022a), in line with the recommendation of Liu et al. (2022), is necessary for the enhanced predictability of climate variables such as precipitation and temperature. This is because the multi-scale interaction between synoptic and inter-annual signals is connected by tropical and extratropical atmospheric signals affecting these CTs, on the intraseasonal time scales.

The majority of the studies linking atmospheric circulations to the climate of southern Africa are focused on precipitation (Barimalala et al., 2020; Fauchereau et al., 2009; Jury, 2015). Other studies have equally examined the relationship between climate drivers and precipitation variability in southern Africa (Hart et al., 2013; Hoell et al., 2015; Reason and Jagadheesha, 2005). Indeed, the studies concur that the hydroclimate of southern Africa is modulated by large-scale circulations. However, little attention has been given to the relationship between synoptic to large-scale circulations in southern Africa and temperature anomalies in southern African landmass. Among such studies, Gillet et al. (2006) investigated the relationship between the SAM and temperature in Southern Hemisphere landmasses. The authors found that positive SAM can be related to temperature increases over the southwestern parts of southern Africa, but temperature decreases over some northeastern parts. The results from Gillet et al. (2006) are consistent with the regression analysis between annual temperature anomalies and the SAM index in this study (Fig. 5). Also, the circulations through which positive SAM increases temperature of the southwestern parts of southern Africa (i.e., CT3+) is shown to be a poleward shift of westerly winds, which in turn suppresses the passage of cold fronts over the southwestern parts of southern Africa. The positive IOD increases SST over the tropical western Indian Ocean (Saji, 1999) and alters atmospheric circulations over southern Africa (Mantasa et al. 2011). Our results indicate that the SST pattern of the positive IOD is linked to temperature increase over Madagascar, the northeastern, northwestern and southwestern parts of southern Africa. Similarly, during El Niño and positive SIOD events, which are both associated with SST increase in the southwest Indian Ocean, temperature increase in some central parts of southern Africa can be expected. Also, El Niño and the positive SIOD appears to be related to temperature decreases over the southwestern parts of southern Africa possibly due to weakening of high-pressure adjacent to South Africa.

A previous study by Ibebuchi (2022b) investigated the effects of climate change on the atmospheric circulation types in southern Africa; it was found that under future climate change the frequency of occurrence, amplitude and spatial configuration of the classified CTs in this work are expected to change. Consequently, the relationship between atmospheric circulations over southern Africa and temperature variability will be impacted by climate change. As documented in Ibebuchi (2023), CMIP6 climate models projected summer periods of weaker circulation at the western branch of the Mascarene high due to warmer southwest Indian Ocean temperatures (i.e., CT4-) as well as summer periods of stronger circulation at the western branch of the Mascarene high due to a more positive SAM (i.e., CT3+). As shown in Figure 2a, a more positive SAM i.e., CT4+ (warmer southwest Indian Ocean i.e., CT3-) will imply warmer temperatures over the southwestern (southeastern) parts of southern Africa.

The climate of Southern Africa is influenced by a complex interplay of feedbacks between the atmosphere and surface processes. Changes in vegetation cover can impact the surface albedo, surface roughness, and evapotranspiration rates, which affect the temperature patterns in a region (e.g., Tran et al. 2017). For example, Clark and Arritt (1995) reported that vegetative cover can have a direct influence on increasing convective precipitation, by not only providing shade to reduce the conduction of heat into the soil (and thus increasing available heat energy in the atmosphere), but also via the extraction of soil moisture. Moreover, a study by Engelbrecht et al. (2015) used a regional climate model to project future temperature changes in Africa, finding that in (southern) Africa as temperature increases, the soils become drier through enhanced evaporation; and this, in turn, impacts vegetation.

Conclusions

This study investigated the mechanisms through which synoptic circulations control atmospheric layer thickness, temperature, relative and specific humidity in southern Africa, during the austral summer season. We also examined the impact of the SAM, IOD, ENSO and SIOD on temperatures in southern Africa. Our results on the synoptic circulations that modulate summer temperature in southern Africa can be summarized as follows:

- The temperature in southern Africa exhibits spatial heterogeneity under the classified CTs. Thus, the distinct regional climate zones within the southern

African landmass contribute to defining the spatial variations of temperature anomalies under a given CT.

- Generally, two asymmetric variabilities in the semi-permanent high-pressure system influence regional temperature variations in southern Africa. First is when the South Atlantic Ocean high pressure is closed, and ridges at the southern coast of southern Africa; this synoptic circulation pattern is associated with the southeast wind to the southern parts of southern Africa from the ridging high pressure and causes cold air advection and negative temperature anomalies in the southern tip of southern Africa. Conversely, when the South Atlantic high is weak on the southern coast of southern Africa, westerly winds dominate over the southern coast of southern Africa, the thickness anomaly value is positive, and the temperature anomaly is positive in the southern parts of southern Africa. Second, when the anticyclonic circulation at the western branch of the Mascarene high is stronger, cold air advection by southeast winds is enhanced into large parts of southern Africa, reducing the atmospheric thickness layer and resulting in negative temperature anomalies. Conversely, when the anticyclonic circulation at the western branch of the Mascarene high is weak during the summer season, atmospheric blocking of the low-pressure system from the tropics is weakened as well, allowing enhanced cyclonic/convective activity in the southwest Indian Ocean; the implication is enhanced warm air advection into parts of southern Africa, increased thickness and positive temperature anomalies in parts of southern Africa. Hence when conditions are favorable, southeast winds from the semi-permanent high-pressure systems are mostly associated with colder temperatures in southern Africa.

- Other variabilities that modulate summer temperature anomalies in southern Africa and interfere with circulations in the high-pressure systems are the formation of continental lows and the trough in the Mozambique Channel. Continental lows increase instability at the boundary layer, increase thickness, and summer temperature anomalies. Further, the strengthening of the Mozambique Channel trough coupled with a weak South Atlantic anticyclone at the southern coast of southern Africa can be implicated to cause widespread warming over South Africa. This is because the aforementioned circulation pattern (i.e., CT9 −) increases the pressure gradient between Mascarene high and the low pressure in the Mozambique Channel so that cold air advection to South Africa is significantly limited.
- Overall, at the synoptic scale, summer temperature anomalies in Madagascar are modulated by cold advection from the Mascarene high and warm advection resulting from a weaker Mascarene high and warmer southwest Indian Ocean waters.
- Climate drivers such as SAM, ENSO, IOD and the SIOD impact temperatures over southern Africa. El Niño and positive SIOD are associated with temperature increase over the central parts of southern Africa. Positive SAM and positive IOD are associated with temperature increase over the southwestern parts of southern Africa, while additionally positive IOD is linked to temperature increase over the northwestern and northeastern parts of southern Africa.

Declarations

Conflict of interest: There are no conflicts of interest in this paper.

Funding statement: This research received no specific grant from any funding agency in the public, commercial, or not-for-profit sectors.

Author's Contribution: All authors worked together on all aspects of the manuscript

Availability of data and material: ERA5 data are available at https://cds.climate.copernicus.eu/cdsapp#!/dataset. The CPC data is available at https://psl.noaa.gov/data/gridded/data.cpc.globaltemp.html

Ethics approval: No human subject is involved in this study and Figures belong to the authors. The paper is also not under consideration in any Journal. There is also no conflict of interest in this paper

Consent to participate: No human research is used. The authors' consent for this paper to be considered

Consent for publication: The authors' consent for this paper to be published.

Reference

Alimonti, G., L. Mariani, F. Prodi, Ricci, R.A., 2022: A critical assessment of extreme events trends in times of global warming. Eur. Phys. J. Plus 137, 1–20.

Allen, M.J., Lee, C.C., 2014: Investigating high mortality during the cold season: mapping mean weather patterns of temperature and pressure. Theor. Appl. Climatol. 118, 419–428.

Barimalala, R., Blamey, R.C., Desbiolles, F., Reason, C.J., 2020: Variability in the Mozambique Channel Trough and impacts on southeast African rainfall. J. Clim. 33, 749–765.

Baudoin, M.-A., Vogel, C., Nortje, K., Naik, M., 2017: Living with drought in South Africa: lessons learnt from the recent El Niño drought period. Int. J. Disaster Risk Reduct. 23, 128–137.

Behera, S.K., Yamagata, T., 2001: Subtropical SST dipole events in the southern Indian Ocean. Geophys. Res. Lett. 28, 327–330.

Benjamini, Y. & Yekutieli, D. 2001: The control of the false discovery rate in multiple testing under dependency. Annals of statistics, 1165-1188.

Burls, N.J., Blamey, R.C., Cash, B.A., Swenson, E.T., Fahad, A. al, Bopape, M.-J.M., Straus, D.M., Reason, C.J., 2019: The Cape Town "Day Zero" drought and Hadley cell expansion. Npj Clim. Atmospheric Sci. 2, 1–8.

Clark, C. A., Arritt, P. W., 1995: Numerical simulations of the effect of soil moisture and vegetation cover on the development of deep convection. Journal of Applied Meteorology and Climatology, 34, 2029-2045.

Compagnucci, R.H., Richman, M.B., 2008: Can principal component analysis provide atmospheric circulation or teleconnection patterns? Int. J. Climatol. J. R. Meteorol. Soc. 28, 703–726.

Dieppois, B., Rouault, M., New, M., 2015: The impact of ENSO on Southern African rainfall in CMIP5 ocean atmosphere coupled climate models. Clim. Dyn. 45, 2425–2442.

Ding, Q., Steig, E.J., Battisti, D.S., Wallace, J.M., 2012: Influence of the tropics on the southern annular mode. J. Clim. 25, 6330–6348.

Engelbrecht, F., Adegoke, J., Bopape, M.J., Naidoo, M., Garland, R., Thatcher, M., McGregor, J., Katzfey, J., Werner, M., Ichoku, C. and Gatebe, C., 2015: Projections of rapidly rising surface temperatures over Africa under low mitigation. Environmental Research Letters, 10,p.085004.

Engelbrecht, C.J., Landman, W.A., 2016: Interannual variability of seasonal rainfall over the Cape south coast of South Africa and synoptic type association. Clim. Dyn. 47, 295–313.

Engelbrecht, C.J., Landman, W.A., Engelbrecht, F.A., Malherbe, J., 2015: A synoptic decomposition of rainfall over the Cape south coast of South Africa. Clim. Dyn. 44, 2589–2607.

Fauchereau, N., Pohl, B., Reason, C.J.C., Rouault, M., Richard, Y., 2009: Recurrent daily OLR patterns in the Southern Africa/Southwest Indian Ocean region, implications for South African rainfall and teleconnections. Clim. Dyn. 32, 575–591.

Flato, G., Marotzke, J., Abiodun, B., Braconnot, P., Chou, S.C., Collins, W., Cox, P., Driouech, F., Emori, S., Eyring, V., 2014: Evaluation of climate models, in: Climate Change 2013: The Physical Science Basis. Contribution of Working Group I to the Fifth Assessment Report of the Intergovernmental Panel on Climate Change. Cambridge University Press, pp. 741–866.

Gillett, N.P., Kell, T.D., Jones, P.D., 2006: Regional climate impacts of the Southern Annular Mode. Geophys. Res. Lett. 33.

Hart, N.C., Reason, C.J., Fauchereau, N., 2013: Cloud bands over southern Africa: Seasonality, contribution to rainfall variability and modulation by the MJO. Clim. Dyn. 41, 1199–1212.

Hendon, H.H., Thompson, D.W., Wheeler, M.C., 2007: Australian rainfall and surface temperature variations associated with the Southern Hemisphere annular mode. J. Clim. 20, 2452–2467.

Hersbach, H., Bell, B., Berrisford, P., Hirahara, S., Horányi, A., Muñoz-Sabater, J., Nicolas, J., Peubey, C., Radu, R., Schepers, D., 2020: The ERA5 global reanalysis. Q. J. R. Meteorol. Soc. 146, 1999–2049.

Hoell, A., Funk, C., Magadzire, T., Zinke, J., Husak, G., 2015: El Niño–Southern Oscillation diversity and southern Africa teleconnections during austral summer. Clim. Dyn. 45, 1583–1599.

Ibebuchi, C.C., 2021a: On the relationship between circulation patterns, the southern annular mode, and rainfall variability in Western Cape. Atmosphere 12, 753.

Ibebuchi, C.C., 2021b: Revisiting the 1992 severe drought episode in South Africa: the role of El Niño in the anomalies of atmospheric circulation types in Africa south of the equator. Theor. Appl. Climatol. 146, 723–740

Ibebuchi, C. C. 2022a. Circulation type analysis of regional hydrology: the added value in using CMIP6 over CMIP5 simulations as exemplified from the MPI-ESM-LR model. Journal of Water and Climate Change, 13(2), 1046-1055.

Ibebuchi, C. C., 2022b: Future trends in atmospheric circulation patterns over Africa south of the equator. Journal of Water and Climate Change, 13, 4194-4212.

Ibebuchi, C. C., 2022c: Can synoptic patterns influence the track and formation of tropical cyclones in the Mozambique Channel? AIMS Geosciences, 8,33-51

Ibebuchi, C.C., 2023a: Circulation patterns linked to the positive sub-tropical Indian Ocean dipole. Adv. Atmospheric Sci. 40, 110–128.

Ibebuchi, C.C., 2023b: Patterns of atmospheric circulation linking the positive tropical Indian Ocean dipole and southern African rainfall during summer. J Earth Syst Sci 132, 13

Jury, M.R., 2015: Passive suppression of South African rainfall by the Agulhas Current. Earth Interact. 19, 1–14.

Knittel, N., Jury, M.W., Bednar-Friedl, B., Bachner, G., Steiner, A.K., 2020: A global analysis of heat-related labour productivity losses under climate change—implications for Germany's foreign trade. Clim. Change 160, 251–269.

Lee, C.C., Sheridan, S.C., 2018: A new approach to modeling temperature-related mortality: Non-linear autoregressive models with exogenous input. Environ. Res. 164, 53–64.

Lee, C.C., Sheridan, S.C., Lin, S., 2012: Relating weather types to asthma-related hospital admissions in New York State. EcoHealth 9, 427–439.

Lennard, C., Hegerl, G., 2015: Relating changes in synoptic circulation to the surface rainfall response using self-organising maps. Clim. Dyn. 44, 861–879.

Liu, F., Wang, B., Ouyang, Y. et al. Intraseasonal variability of global land monsoon precipitation and its recent trend. npj Clim Atmos Sci 5, 30 (2022). https://doi.org/10.1038/s41612-022-00253-7,

Lyon, B., Mason, S.J., 2007: The 1997–98 summer rainfall season in southern Africa. Part I: Observations. J. Clim. 20, 5134–5148.

Mahlalela, P.T., Blamey, R.C., Reason, C.J.C., 2019: Mechanisms behind early winter rainfall variability in the southwestern Cape, South Africa. Clim. Dyn. 53, 21–39.

Malherbe, J., Landman, W.A., Engelbrecht, F.A., 2014: The bi-decadal rainfall cycle, Southern Annular Mode and tropical cyclones over the Limpopo River Basin, southern Africa. Clim. Dyn. 42, 3121–3138.

Manatsa, D., Matarira C. H., Mukwada G. 2011: Relativeimpacts of ENSO and Indian Ocean dipole/zonal mode oneast SADC rainfall. Int J Climatol 31, 558–577. https://doi.org/10.1002/joc.2086

Manatsa, D., Mushore, T., Lenouo, A., 2017: Improved predictability of droughts over southern Africa using the standardized precipitation evapotranspiration index and ENSO. Theor. Appl. Climatol. 127, 259–274.

Morioka, Y., Takaya, K., Behera, S.K., Masumoto, Y., 2015: Local SST impacts on the summertime Mascarene high variability. J. Clim. 28, 678–694.

Pirhalla, D.E., Lee, C.C., Sheridan, S.C., Ransibrahmanakul, V., 2022: Atlantic coastal sea level variability and synoptic-scale meteorological forcing. J. Appl. Meteorol. Climatol. 61, 205–222.

Reason, C.J.C., 2001: Subtropical Indian Ocean SST dipole events and southern African rainfall. Geophys. Res. Lett. 28, 2225–2227.

Reason, C.J.C., Jagadheesha, D., 2005: A model investigation of recent ENSO impacts over southern Africa. Meteorol. Atmospheric Phys. 89, 181–205.

Reason, C.J.C., Rouault, M., 2005: Links between the Antarctic Oscillation and winter rainfall over western South Africa. Geophys. Res. Lett. 32.

Roffe, S. J., van der Walt, A. J. 2023: Representation and evaluation of southern Africa's seasonal mean and extreme temperatures in the ERA5-based reanalysis products. Atmospheric Research, 284, 106591.

Saji, N. H. et al., 1999: A dipole mode in the tropical Indian Ocean. Nature 401:360-363.

Sheridan, S.C., Allen, M.J., 2015: Changes in the frequency and intensity of extreme temperature events and human health concerns. Curr. Clim. Change Rep. 1, 155–162.

Sheridan, S.C., Dixon, P.G., 2017: Spatiotemporal trends in human vulnerability and adaptation to heat across the United States. Anthropocene 20, 61–73.

Sheridan, S.C., Lee, C.C., 2018: Temporal trends in absolute and relative extreme temperature events across North America. J. Geophys. Res. Atmospheres 123, 11,889-11,898.

Sheridan, S.C., Lee, C.C., Allen, M.J., 2019: The mortality response to absolute and relative temperature extremes. Int. J. Environ. Res. Public. Health 16, 1493.

Silvestri, G., Vera, C., 2009: Nonstationary impacts of the southern annular mode on Southern Hemisphere climate. J. Clim. 22, 6142–6148.

Tran, D. X., Pla, F., Latorre-Carmona, P., Myint, S. W., Caetano, M., Kieu, H. V., 2017: Characterizing the relationship between land use land cover change and land surface temperature. ISPRS Journal of Photogrammetry and Remote Sensing, 124, 119-132.

Vigaud, N., Richard, Y., Rouault, M., Fauchereau, N., 2009: Moisture transport between the South Atlantic Ocean and southern Africa: relationships with summer rainfall and associated dynamics. Clim. Dyn. 32, 113–123.

Wolski, P., Jack, C., Tadross, M., van Aardenne, L., Lennard, C., 2018: Interannual rainfall variability and SOM-based circulation classification. Clim. Dyn. 50, 479–492.

FIGURES

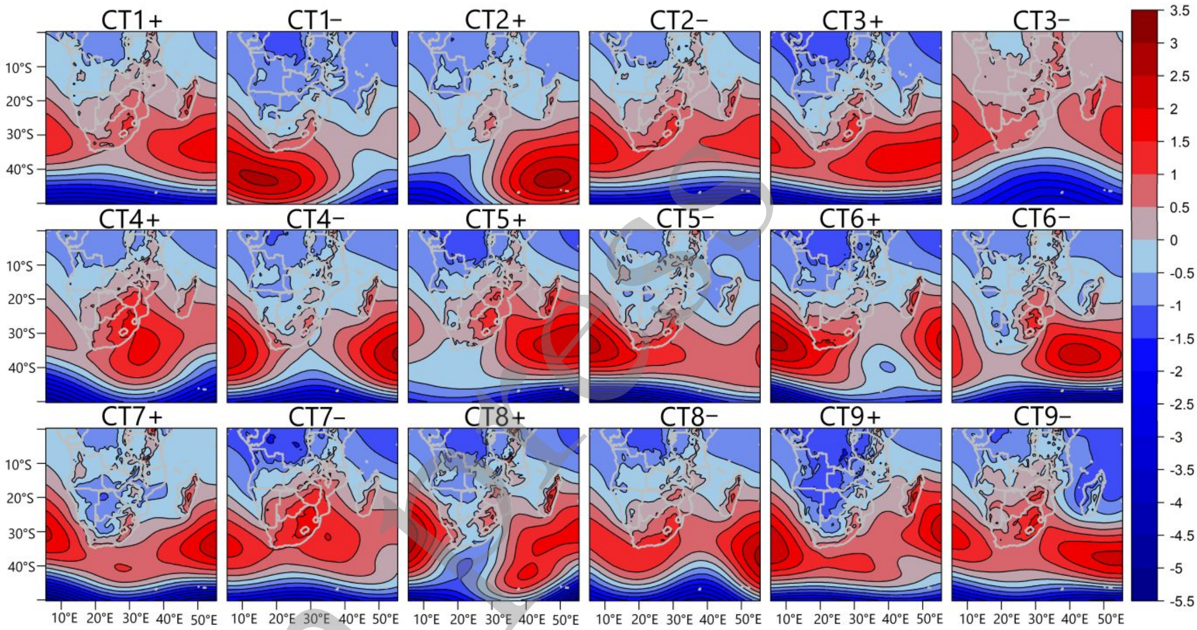

Fig. 1 z-score standardized SLP composite of the classified CTs

a)

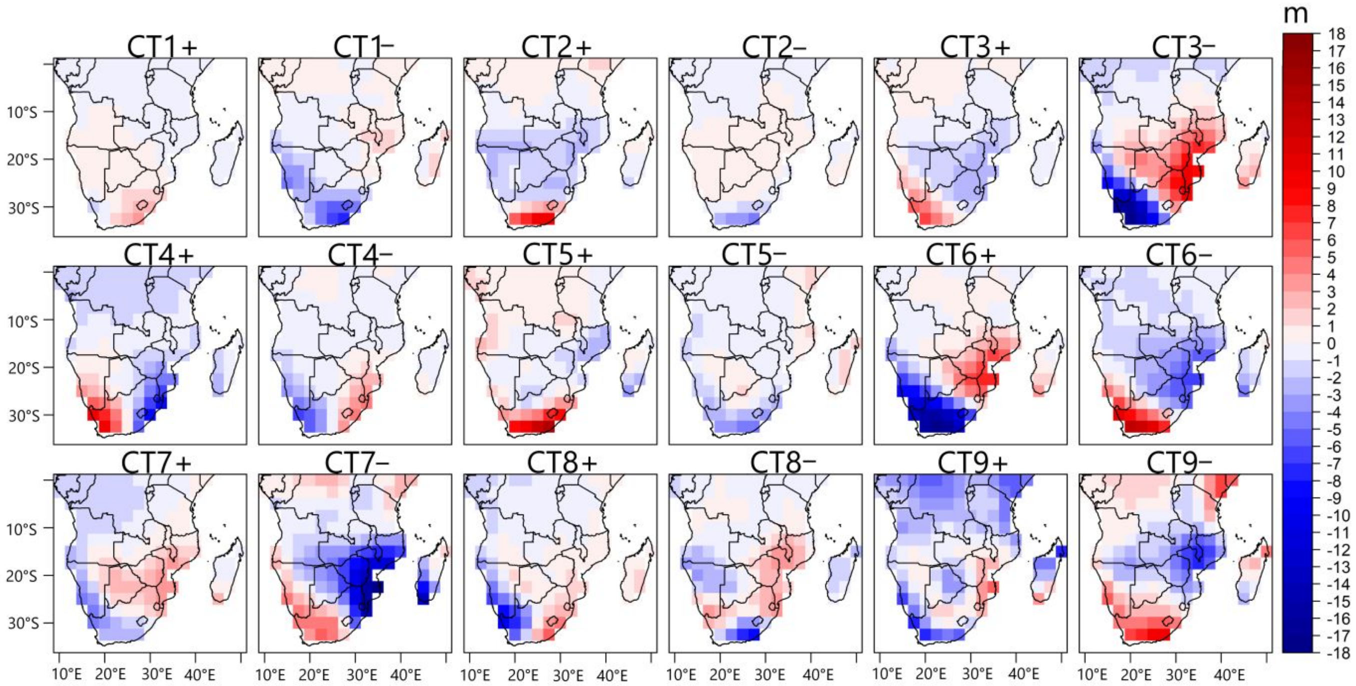

b)

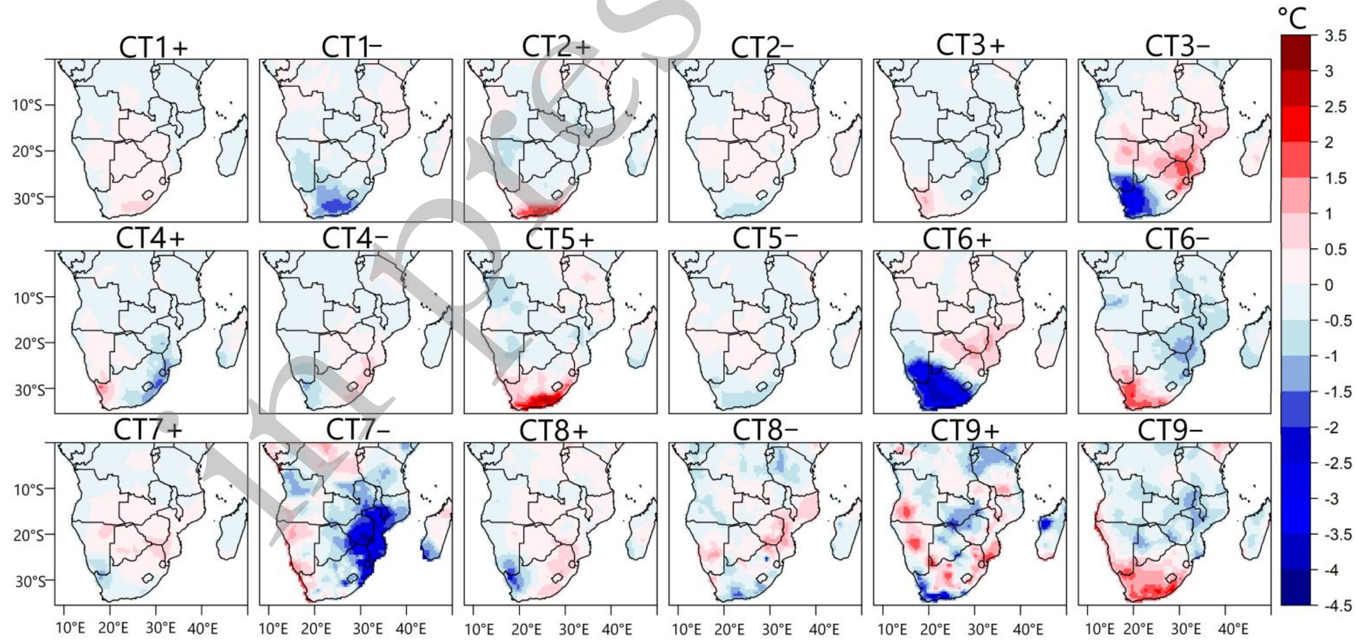

Fig. 2 Standardized composite anomaly maps of thickness layer between 1000 hPa and 850 hPa (a) and 2 m temperature anomaly during DJF for the classified CTs in Fig. 1

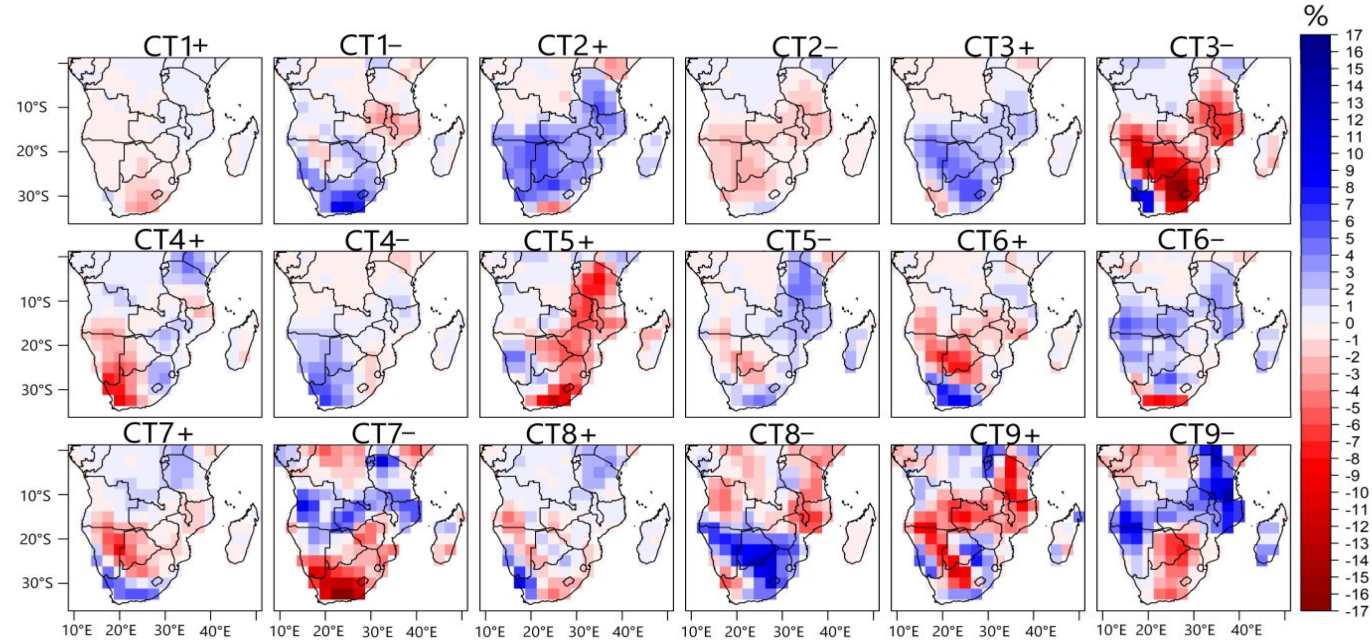

Fig. 3 Standardized composite anomaly maps of 850 hPa relative humidity during DJF for the classified CTs in Fig. 1

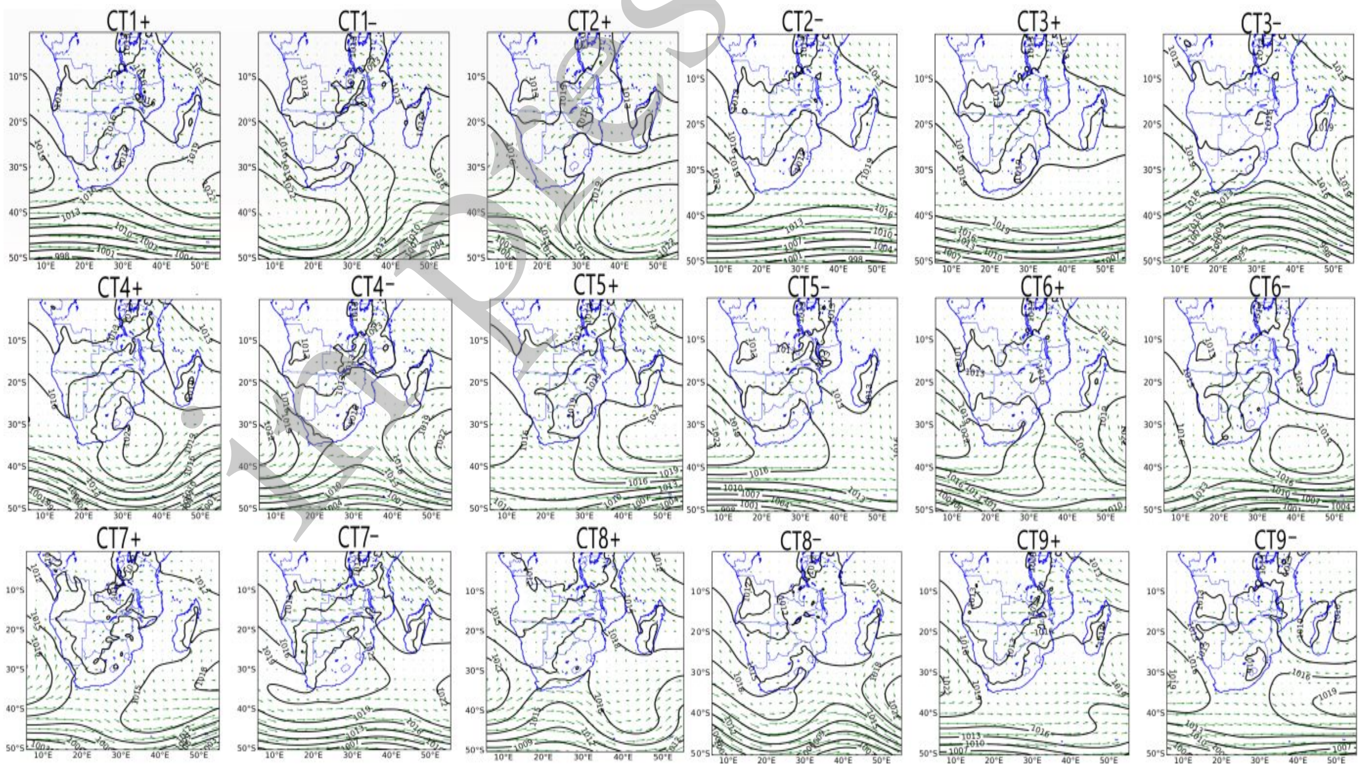

Fig. 4 Composite maps of SLP (black contours) and 850 hPa wind (green vectors) for the classified CTs in Fig. 1. The Contour interval is 3 hPa

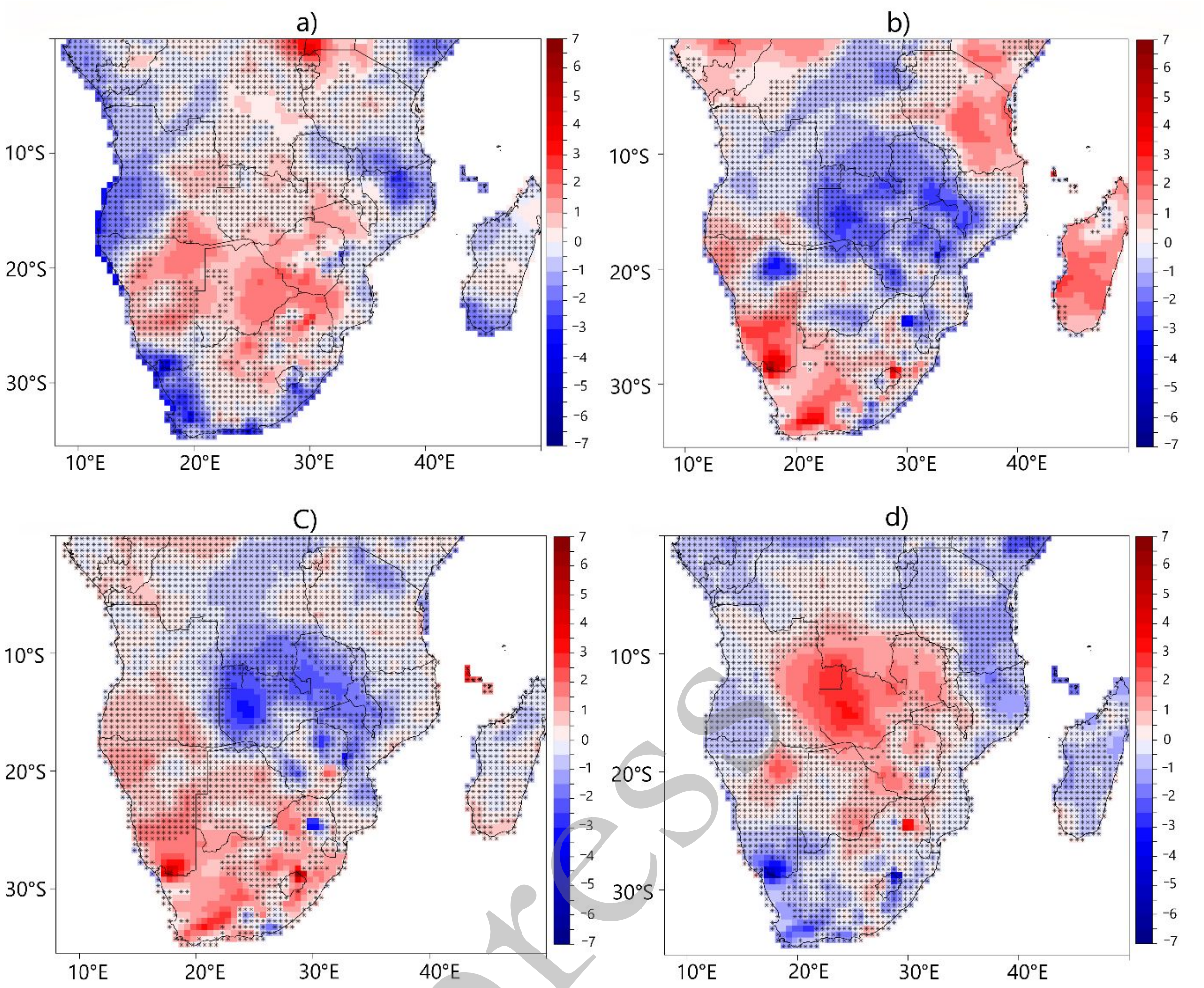

Fig. 5 Regression map of a) Nino 3.4 index; b) IOD index; c) SAM index; and d) SIOD index d) onto annual mean temperature anomaly in southern Africa from 1979 to 2021. Stippling shows grid points that are not statistically significant at a 95% confidence level.

Appendix A

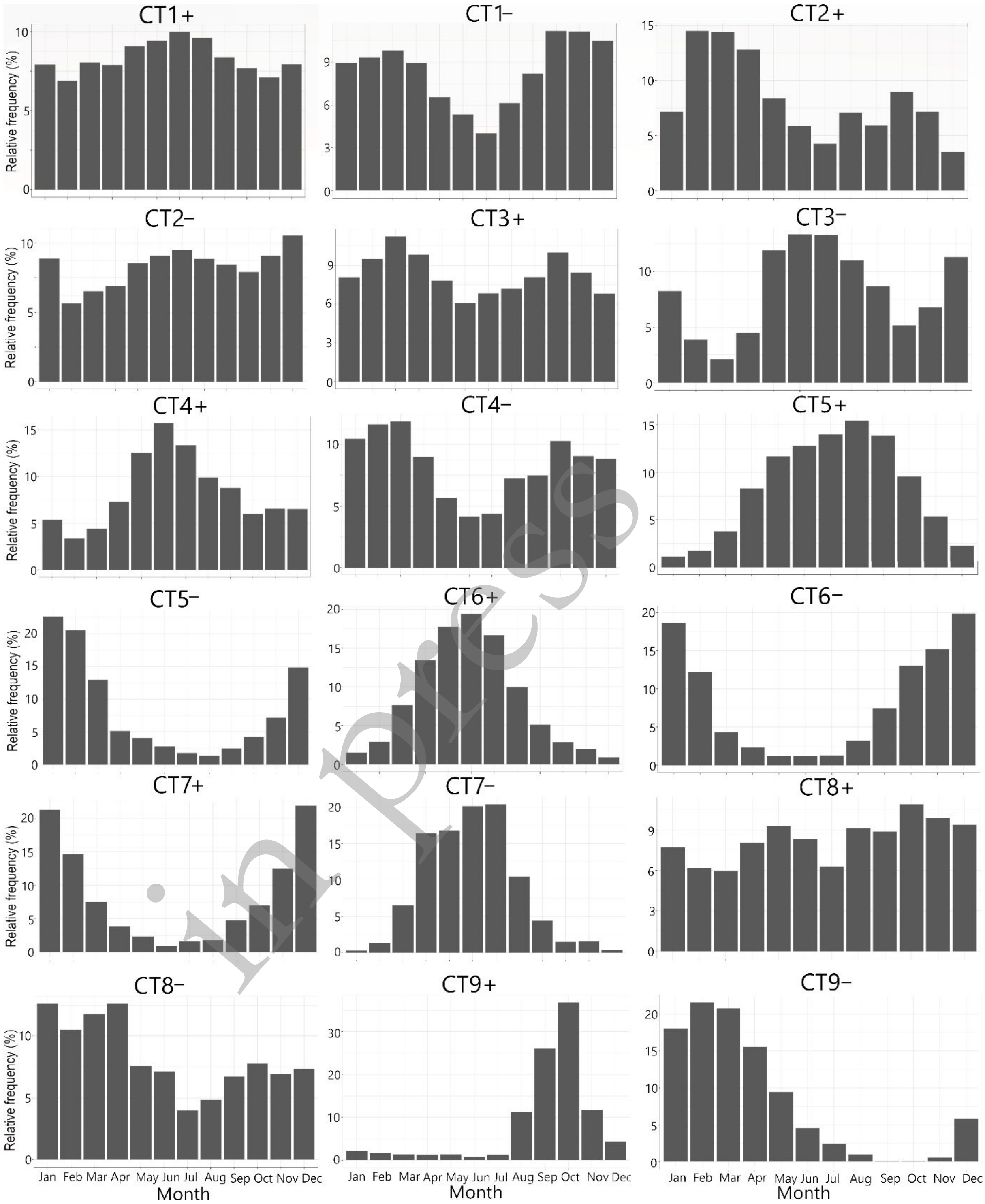

Fig. A1 Annual cycle of the CTs in Fig. 1. Y axis is the relative frequency of occurrence of the CTs and the x-axis is the twelve calendar months in a year.

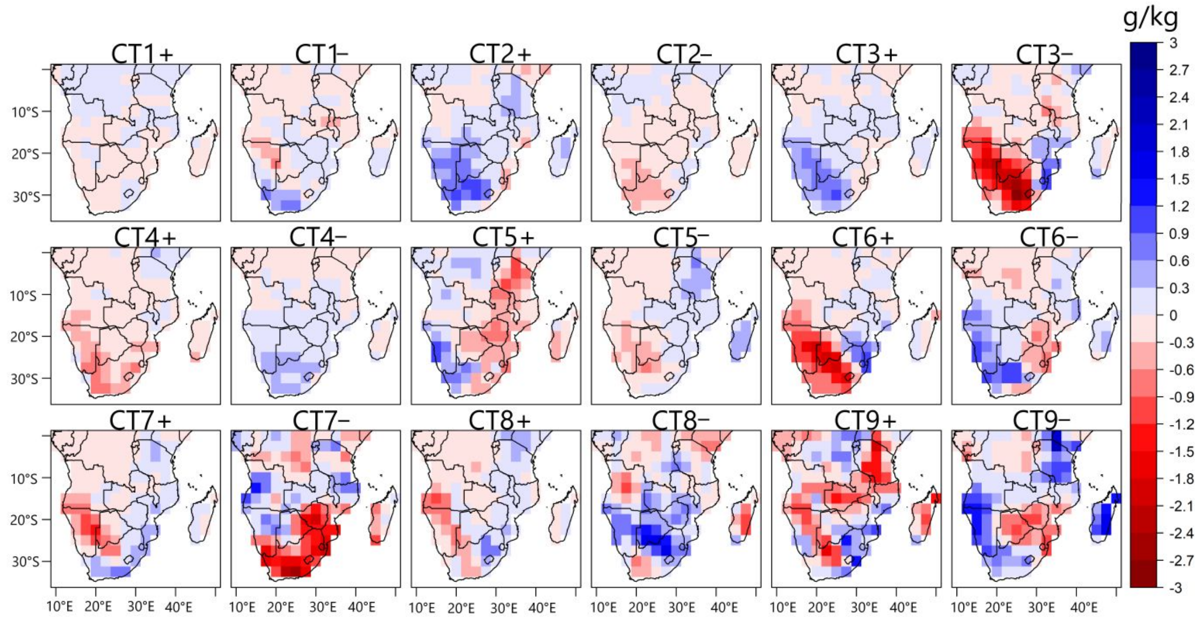

Fig. A2 Standardized composite anomaly maps of 850 hPa specific humidity during DJF for the CTs in Fig. 1

<u>Classification of circulation types using the obliquely rotated T-mode PCA</u>

The classification of the CTs is completely eigenvector-based (Richman 1981, 1986). It involves the application of obliquely rotated PCA to the T-mode matrix (variable or column matrix is time series and row matrix is grid points) of z-score standardized SLP field. The SLP field is standardized to give equal weight to all days in the analysis period. Singular value decomposition is applied to the correlation matrix, containing the correlation between SLP observations at each time in the analysis period, to obtain the PC scores, eigenvalues, and eigenvectors. The PC scores capture the spatial variability patterns, and the eigenvectors localize the spatial patterns in time. To make the eigenvectors responsive to rotation and to become correlations between the PC scores and the standardized SLP field, the eigenvectors are multiplied by the square root of their corresponding eigenvalues so that they become PC loadings that can be longer than a unit length. To enhance the physical interpretability of the PC loadings they were rotated obliquely using Promax at a power of 2. The oblique rotation simplifies the structure of the PCs by maximizing the number of near-zero loadings, so that unique time series with large loading magnitudes are clustered under a given PC. Given that we desire to analyse both dominant and (rare) patterns associated with extremes, of which the latter is often located in higher order PCs, we decide on the optimal number of PCs to retain and rotate by iteratively increasing the number of PCs until the next added PC is least unique from the already retained PCs. Since each PCs contains asymmetric patterns separated by the sign of the PC loadings, following its efficacy, in previous studies, ± 0.2 is used in this study to separate PC loadings in the signal range from PC loadings in the noise range. Introducing the threshold allows a day can be classified under more than one PC pattern insofar as the PC has signal magnitude $>|0.2|$ on that day. Hence each retained PC gives two asymmetric classes (i.e., clusters above and below the ± 0.2 threshold) and the SLP mean of the days in a given class is the CT.